NTNU

Norwegian University of
Science and Technology

Optimization of Operation and Remaining Lifetime of a Subsea System

Morten Aulin Moen

Chemical Engineering and Biotechnology
Submission date: June 2016
Supervisor: Johannes Jäschke, IKP
Co-supervisor: Adriaen Verheyleweghen, IKP

Norwegian University of Science and Technology
Department of Chemical Engineering

Preface

This thesis was written as the final work of the master program in Chemical Engineering at the Norwegian University of Science and Technology.

I would like to express my deep gratitude to my supervisor associate professor Johannes Jäschke for helpful guidance, enthusiastic encouragement and useful critiques during this project. I would like to express my very great appreciation to my co-supervisor phd candidate Adriaen Verheyleweghen for helpful feedback and lively discussions.

Declaration of Compliance

I hereby declare the this thesis is an independent work in agreement with the exam rules and regulations of the Norwegian University of Science and Technology.

Trondheim, 27.06.2016

Morten Aulin Moen

Abstract

A model of a subsea system was developed and optimization for operation and remaining life time. For the modelling of the remaining life time the compressor efficiency was used as there is no statistical or physical model available. Before the optimization was performed a degree of freedom analysis were executed, and it was found that 3 variables could be used for control. For the optimization four cases was examined. In the three first cases the objective function was changed. In the fourth case uncertainty was included and for handling the uncertainty chance-constraint was used. All of the calculation was done in Python 2.7 and the optimal control problem was formulated in CasADi 3.0. Optimization result from case 1 yielded 3 active constraint, these constraint was also active in all of the other cases. The lower bound the compressor efficiency which restricted the overall gas production. The upper bound on the mass fraction of gas in stream 3, which restricted the separation efficiency. The lower bound on the pressure in stream 6 was reached because of degeneration of the compressor efficiency. For case 2 the end time was included as a free variable. From the result of case 2 the upper bound on the end time was reached, as lower daily production of gas gave better separation. In case 3 the net present value of the gas was included in the objective function. In case 3 the optimizer found it advantageous to maximize the gas production in the beginning, which caused the time horizon to be reduced. For case four uncertainty in the reservoir flow coefficient was included for the optimization. For solving the optimal control problem with uncertainty chance-constraint was used. Chance-constraint was included on the lower bound on the compressor efficiency at the end of the time horizon and the upper bound on the mass fraction of gas in stream 3. The optimization result gave a higher probability of holding the constraint than the probability level. But calculating new back-offs and solving the optimal control problem again the probability of holding the constraint started to converge towards the probability level. With uncertainty in the optimization problem chance-constraint can be used. With chance-constraint the probability of constraint violation can be decided such that the back-off is reduced.

Table of Contents

List of Tables

List of Figures

Abbreviations

CV	=	Control variable
GOR	=	Gas oil ratio
MPC	=	Model predictive control
MV	=	Manipulated Variable
NPV	=	Net present value
OCP	=	Optimal control problem
PDF	=	Probability distribution function
RMPC	=	Robust model predictive control
SMPC	=	Stochastic model predictive control
SOCP	=	Stochastic optimal control problem

List of Symbols

Symbol	Unit	Description
Δt_k	d	Length of time period k
η	-	Compressor efficiency
γ	-	heat capacity
$\mathbf{\Phi}$	-	Lagrange term of the objective function
ρ_j	$\mathrm{kt\,m^{-3}}$	Density of component j
σ	-	variance
τ	d	Residence time
ξ	-	Uncertainty with given probability distribution
A	-	Gas damaging factor
B	-	Oil damaging factor
c	-	Lower bound of constraint
C	$\mathrm{bar\,d^{-1}}$	Reservoir degeneration factor
C_f	-	Cash flow
C_v	$\mathrm{kt\,d^{-1}\,bar^{0.5}}$	Valve coefficient
$f(y)$	-	Valve characteristic function
$\mathbf{f}$	-	Differential equations
F_g	-	Gaussian distribution function
g	$\mathrm{m\,d^{-2}}$	Gravitational constant
$\mathbf{g}$	-	Algebraic equations
dh	m	Height between reservoir and seabed
h	m	liquid height in the separator
H	-	Constraint vector
i	-	Interest rate
J	$\mathrm{m\,d^{-1}\,bar^{-1}}$	Flow coefficient

k_i	$\mathrm{kt\,d^{-1}\,bar^{-2n}}$	Flow coefficient for component i
L	m	Length of the separator
$\dot{m}_{j,i}$	$\mathrm{kt\,d^{-1}}$	Mass flow in stream j for component i
$\dot{m}_{j,i_{max}}$	$\mathrm{kt\,d^{-1}}$	Maximum mass flow in stream j for component i
M_i	$\mathrm{kt\,kmole^{-1}}$	Molar weight of component i
n	-	Deliverability exponent
N	-	Number of time periods
p	-	Price of gas
$\mathbf{p}$	-	Parameter vector
p_n	-	normal distribution function
PV	-	Present Value
P_r	bar	Reservoir pressure
P_{wf}	bar	Well bore-head pressure
q	$\mathrm{m^3\,d^{-1}}$	Volumetric flow
R	m	Radius of the separator
R_g	$\mathrm{MW\,K^{-1}\,kmole^{-1}}$	Universal gas constant
S_i	d	Separation efficiency of component i
SG_j	-	Specific gravity of stream j
t_f	d	End time for the time horizon in days
T	k	Temperature
$\mathbf{u}_{lb}$	-	Lower bound for control variables
$\mathbf{u}_{ub}$	-	Upper bound for control variables
$\mathbf{u}_k$	-	Control variable vector at time step k
V_g	$\mathrm{m^3}$	Volume of gas phase in the separator
V_{sep}	$\mathrm{m^3}$	Volume of the separator
W	MW	Compressor duty
W_s	MW	Specific Work
$\mathbf{x}_{lb}$	-	Lower bound for differential variables
$\mathbf{x}_{ub}$	-	Upper bound for control variables
$\mathbf{x}_k$	-	Differential variable vector at time step k

y	-	Random variable
$\bar{y}$	-	Mean value of y
$\mathbf{Y}$		Covariance matrix for y
$\mathbf{z}_{lb}$	-	Lower bound for algebraic variables
$\mathbf{z}_{ub}$	-	Upper bound for control variables
$\mathbf{z}_k$	-	Algebraic variable vector at time step k
$Z_{j,i}$	-	Mass fraction of component i in stream j
$\mathbb{E}$	-	Estimation
$\mathbb{P}$	-	Probability

Chapter 1

Introduction

Due to low oil prices the offshore industry are forced to improve the efficiency of operation to remain competitive in the global marked. One of the technologies that has gotten an increased focus from both the industry and the scientific communities, is subsea technology. Subsea technology has shown to improve production, increase expected life-time of the reservoir, decrease processing costs and reduce environmental impact [25] [29]. Furthermore, subsea technology is also looking promising for developing new offshore fields where the climate is harsh and the water depth is high.

On the Norwegian continental shelf, subsea technology has been used for improve the expected life-time and production of fields like Tordis and Troll [11] [25]. Though subsea technology is a mature technology on the Norwegian continental shelf, there are still unsolved problems. One of the problems is that for each field the conditions are unique thus each field is facing unique technological challenges [28] [29]. These challenges need to be identified and addressed when designing a subsea system.

For the daily operation of a subsea system, small changes in operating conditions can have huge effects on the performance of the system. Therefore, finding and keeping the system at the conditions that gives the best performance often translates into large savings. Subsea systems can often consist of multiple processing units [12] [25] [35] with complicated and interacting phenomena occurring. In the chemical industry model predictive control (MPC) have shown good results for controlling system with similar complexity [24] [27]. The MPC solves an open loop optimal control problem (OCP) repeatedly over a receding time horizon for finding the optimal control action sequences. Then the first control sequence is applied and the process is repeated. Therefore needs the model that the MPC uses to accurate predict the future state of the system but also not be to complex or the computational time for solving the OCP will be to high.

The OCP used in the MPC often have an objective function that tries to maximize profit or similar economical objectives. This usually causes the system to be driven towards the

constraints [6]. The system is in reality often subjected to various form of uncertainties, for example measurement noise. Therefore, if the constraints are active these uncertainties can often lead to constraint violations or sub-optimal control sequences. Therefore is it common to add a safety margin (back-off) from the constraints such that the constraints is not violated. This back-off is often found by considering a worst case scenario of the uncertainty [4] [5]. However, this approach often leads to overly conservative control action such that system are kept at sub-optimal conditions. Therefore if the uncertainties in the system are included in the OCP the system can be kept closer to the optimal without causing constraint violations. This would improve the efficiency of operating and make the subsea system more competitive.

For gas field like Snøhvit and Ormen Lange gas compression system is used for increase life-time of the gas field [12] [35]. One of the technological challenges these fields are phasing is when to schedule maintenance of the compressor system. Therefore, in this Master thesis it have been examined how to model a subsea separation system with compression. The optimize the system with considering operation and remaining life time of the compressor. For this purpose, first a model of a subsea system with gas compression was developed. Then the control objective of the system was defined and 3 cases with different objective function of the OCP was examined. Then a fourth case was examined where there was uncertainty in the system and chance constraint was used for handling the uncertainty. The OCP was solved and compared with the previous cases.

This Master thesis is organized as follows: in Chapter 2 general theory about dynamic and stochastic dynamic optimization is presented. Thereafter in Chapter 3 the model of the subsea system is presented. In Chapter 4 it is explained how the OCP is formulated, both with and without uncertainty. In Chapter 5 the four cases that are examined is presented. In Chapter 6 the results of the optimizations are presented and discussed. Finally in Chapter 7 the conclusion along with future work is presented.

Chapter 2

Optimization Theory

The theory of optimization can trace its roots back to the work of Euler and Lagrange with the development of the Euler-Lagrange equation [30] in the 18th century. Further development in the theory of optimization was done by the likes of Gauss and Newton. Research on optimization stayed mostly inside the field of mathematics. Not before Dantzig developed the Simplex method in 1947 [17] did optimization start to get focus from other fields than mathematics. This is often stated as the beginning of modern optimization. Since then a great deal of research and development has been done in the field of optimization. The introduction of dynamics optimization by Bellman in 1954 [3] and development of non-linear solvers like Ipopt [42] are some examples. With these advances, optimization is now often used in fields like economics, engineering and science.

For chemical engineers today optimization have found applications in numerous areas. One of the area of chemical engineering where optimization have yield good results is in process control [6]. As small changes in the operating conditions of process equipment can often have huge effect on the performance of the equipment. Therefore having a systematic approach for finding the conditions which yields the best economical results can help with reducing the expenses. The optimization problems one solves in process control is often called optimal control problems (OCPs). These OCPs include a large variety of optimization problems. The solving method for OCPs differ depending on what kind of optimization problem it is. A common form of OCP is dynamic optimal control. Dynamic optimal control are optimization problems where the optimal changes with time. More about how dynamic optimization and how it works is given in Section 2.1. In process control one often take measurements of the system for calculating the state of the system. The problem with using measurements for calculating the state of the system is that the measurements include some uncertainty. A widespread approach more dealing with this uncertainty of the measurement is to use the expected value [27]. The problem with using the expected value in the optimization is that the optimum one get can be infeasible or not close to the actual optimum [34]. In process control and other field there have been a lot of work on including the uncertainty of the measured values or other kind of uncertainties into

the optimization formulation [26]. When the uncertainty is included into the optimization problem the problem becomes stochastic. More about dynamic stochastic optimization is given in Section 2.2.

2.1 Dynamic Optimization

Before going into the theory of dynamic optimization lets us first start with some notation and how to formulate a general dynamic optimization problem. This is done since the notation and formulation often differ depending on the field of studies [6], [30].

Assume that the dynamics system that is going to be optimized can be modelled by a set of differential-algebraic equations (DAEs). Furthermore assume that the problem can be expressed as an initial value problem. For control one often has knowledge of the initial state of the system, so the assumption that the problem can be expressed as an initial value problem is reasonable [6]. With these assumption the set of DAEs can be expresses as:

$$\frac{d\mathbf{x}}{dt} = \mathbf{f}\left(\mathbf{x}(t), \mathbf{z}(t), \mathbf{u}(t), \mathbf{p}\right) \tag{2.1a}$$

$$\mathbf{x}(0) = \mathbf{x_0} \tag{2.1b}$$

$$\mathbf{g}\left(\mathbf{x(t)}, \mathbf{z(t)}, \mathbf{u(t)}, \mathbf{p}\right) = 0 \tag{2.1c}$$

In the equation above $\mathbf{f}$ are the differential equations and $\mathbf{g}$ are the algebraic equations. $\mathbf{x}(t) \in \mathbb{R}^{n_x}$ are the differential variables, $\mathbf{x_0}$ are the initial values at time equal to zero, $\mathbf{z}(t) \in \mathbb{R}^{n_z}$ are the algebraic variables, $\mathbf{u}(t) \in \mathbb{R}^{n_u}$ are the control variables and $\mathbf{p} \in \mathbb{R}^{n_p}$ are the parameters that are independent of t.

For the set of DAEs given in Equation (2.1) let us assume that with given values of $\mathbf{x}(t)$, $\mathbf{u}(t)$ and $\mathbf{p}$, $\mathbf{z}(t)$ can be found uniquely by $\mathbf{g}$.

The set of DAEs given in Equation (2.1) are included into the optimization formulation as constraints. This is to make certain that any solution of the optimization problem is a feasible solution of the set of DAEs. The set of feasible solutions of (2.1) may include solutions that are physically infeasible or not inside the safe zone of operation. Because of this, upper and lower bounds on the variables need to be added to the optimization formulation. These bounds can be given by the design of the system, for example maximum temperature inside a reactor. Bounds are also added such that the solutions are physical consistent, for example that all mass fractions are between zero and one. Also a good engineer can use his/her insight to further restrict the feasible set by adding/adjusting bounds, for example that mass fraction of a reactant should be above some minimum value. The lower and upper bounds on the variables are usually expressed as in Equation (2.2) where it is divided by the different type of variables.

$$\mathbf{x_{lb}} \leq \mathbf{x} \leq \mathbf{x_{ub}} \tag{2.2a}$$
$$\mathbf{z_{lb}} \leq \mathbf{z} \leq \mathbf{z_{ub}} \tag{2.2b}$$
$$\mathbf{u_{lb}} \leq \mathbf{u} \leq \mathbf{u_{ub}} \tag{2.2c}$$
$$\tag{2.2d}$$

Here the subscript lb denotes lower bounds and the subscript ub denotes upper bounds.

Then the feasible set contains all the solutions that satisfy the constraints given by Equation (2.1) and the bounds given by Equation (2.2). For the feasible set assume that it is not empty [30], and therefore there exist a least one solution that satisfy both the constraints and variables bounds.

To differentiate the solutions given by the feasible set, an objective function is added. This objective function defines the function that is going to be minimized or maximized. The objective function defines the goal of the optimization for example maximize production of gas for a subsea processing system. Assume that time horizon is bounded, then the objective dunction can be expressed as:

$$\int_0^{t_f} \mathbf{\Phi}\left(\mathbf{x}(t), \mathbf{z}(t), \mathbf{u}(t), \mathbf{p}\right) dt, \tag{2.3}$$

In Equation 2.3 t_f finial value of the time horizon and $\mathbf{\Phi}$ is the Lagrange term of the objective function.

Now with the constraints defined by Equation (2.1), the variables bounds defined by Equation (2.2) and the objective function defined by Equation (2.3), the whole optimization problem formulation can be expressed. Assume that the problem is a minimization problem. The the optimization problem formulation can be expressed as:

$$\min_{\mathbf{u}(t)} \quad \int_0^{t_f} \mathbf{\Phi}\left(\mathbf{x}(t), \mathbf{z}(t), \mathbf{u}(t), \mathbf{p}\right) dt \tag{2.4a}$$
$$s.t. \quad \frac{d\mathbf{x_k}}{dt} = \mathbf{f}\left(\mathbf{x}(t), \mathbf{z}(t), \mathbf{u}(t), \mathbf{p}\right) \tag{2.4b}$$
$$\mathbf{x}(0) = \mathbf{x_0} \tag{2.4c}$$
$$\mathbf{g}\left(\mathbf{x}(t), \mathbf{z}(t), \mathbf{u}(t), \mathbf{p}\right) = 0 \tag{2.4d}$$
$$\mathbf{x_{lb}} \leq \mathbf{x}(t) \leq \mathbf{x_{ub}} \tag{2.4e}$$
$$\mathbf{z_{lb}} \leq \mathbf{z}(t) \leq \mathbf{z_{ub}} \tag{2.4f}$$
$$\mathbf{u_{lb}} \leq \mathbf{u}(t) \leq \mathbf{u_{ub}} \tag{2.4g}$$

The above equation is a general formulation of a dynamic optimization problem, with the notation normally used in process control.

To solve a dynamic optimization problem like the one given in Equation (2.4), Bellman suggested that the problem is divided into finite number sub-problems [3]. Each sub-problem is solved for given time. Such that solution does not get discontinuous from one time period to the next. Bellman added additionally constraints, often called continuity constraints. These constraints stated that at the end of time k the variables is equal to variables at the start of time $k+1$. Equation (2.5) shows such a constraint.

$$\mathbf{x}_{k+1}(0) = \mathbf{x}_k(t_k). \tag{2.5}$$

In the equation above $\mathbf{x}_{k+1}(0)$ are the differential variables at time period $k+1$ at time equal to zero, and $\mathbf{x}_k(t_k)$ are the differential variables at time period k at the end of that time period.

By dividing the time horizon into a finite number of discrete points, the objective function can be approximated by the following Riemann sum:

$$\sum_{k=0}^{N-1} \mathbf{\Phi_k}\left(\mathbf{x}(t_{k+1}), \mathbf{z}(t_{k+1}), \mathbf{u}(t_k), \mathbf{p}\right) \Delta t_k, \tag{2.6}$$

where N is the number of time periods, $\mathbf{x}(t_{k+1})$, $\mathbf{z}(t_{k+1})$ are the values of the differential and algebraic variables at the end of the time period k and Δt_k is the length of the time period k. The values of $\mathbf{x}$ and $\mathbf{z}$ are sampled at t_{k+1} because $\mathbf{X_0}$is assumed to be given, so it is not a decision variable.

By adding the continuity constraint given by Equation (2.5) and the new objective function given by Equation (2.6), the dynamic optimization problem defined by Equation (2.4) can be defined as set of optimization problems. Where the optimization problem defined at time step k is only dependent on the previous time steps. In Equation (2.7) the new dynamics optimization formulation is given, where the time horizon is divided into a finite number of discrete points.

$$\begin{aligned}
\min_{\mathbf{U}} \quad & \sum_{k=0}^{N-1} \mathbf{\Phi_k}\left(\mathbf{x_{k+1}}, \mathbf{z_{k+1}}, \mathbf{u_k}, \mathbf{p}\right) \Delta t_k && \text{(2.7a)}\\
s.t. \quad & \mathbf{x_{k+1}} = \mathbf{f_k}\left(\mathbf{x_k}, \mathbf{z_k}, \mathbf{u_k}, \mathbf{p}\right), \quad \forall\, k = 1, .., N && \text{(2.7b)}\\
& \mathbf{x_{k+1}}(0) = \mathbf{x_k}(t_k), \quad \mathbf{x_0} = \text{given}, \quad \forall\, k = 0, .., N-1 && \text{(2.7c)}\\
& \mathbf{g_k}\left(\mathbf{x_k}, \mathbf{z_k}, \mathbf{u_k}, \mathbf{p}\right) = 0, \quad \forall\, k = 0, .., N && \text{(2.7d)}\\
& \mathbf{x_{lb}} \leq \mathbf{x_k} \leq \mathbf{x_{ub}}, \quad \forall\, k = 1, .., N && \text{(2.7e)}\\
& \mathbf{z_{lb}} \leq \mathbf{z_k} \leq \mathbf{z_{ub}}, \quad \forall\, k = 1, .., N && \text{(2.7f)}\\
& \mathbf{u_{lb}} \leq \mathbf{u_k} \leq \mathbf{u_{ub}}, \quad \forall\, k = 0, .., N-1 && \text{(2.7g)}\\
& && \text{(2.7h)}
\end{aligned}$$

In the equation above notation $\mathbf{y}(t_k)$ is shortened to $\mathbf{y_k}$, where y is one of the variables. This is done so the notation gets more compact.

Before solving the optimization problem defined in Equation (2.7) it is important to define which category of optimization problems the problem belongs in. This is since different optimization problems require different solution approaches. For example, linear problems are commonly solved using the simplex method, whereas non-linear problems are solved using the interior point (IP) method or the sequential quadratic programming (SQP) method. More about the different solving methods can be found in *Numerical Optimization* by Nocedal [6] and in *Nonlinar Programming* by Biegler [30].

2.2 Dynamic Stochastic Optimization

When controlling a system with a MPC the system is often driven to the constraints. In reality there is always some form of uncertainty either from measurements or model mismatch. These uncertainties can often lead to constraint violations or sub-optimal solutions. Therefore have the been done a great deal of research on how handle the uncertainties. The first approach to handle the uncertainties was the use of $\min - \max$ MPC [4] [7] [44]. For the $\min - \max$ MPC approach the solution of the OCP must satisfy all of the possible outcomes of the uncertainties. As the worst case scenario is considered it usually lead to conservative control actions or in some cases infeasible solution [5] [20]. For overcome the limitations of $\min - \max$ MPC, tube-based MPC was developed [20] [32]. Tube-based MPC uses a partially separable feedback control law parameterization such that the uncertainties can be handled directly. Though tube-based MPC could handle the uncertainties directly it is not easily designed for non-linear systems and it can often give conservative control action. Both $\min - \max$ MPC and tube-based MPC falls into the category of robust MPC (RMPC). The problem with RMPC is that it rely on bounded, deterministic descriptions of the uncertainties in measurement or model mismatch. In reality the uncertainties are usually more accurate described as probabilistic functions. Therefore with the uncertainty described by some probability distribution function (PDF) it is natural to include this into the OCP. With the inclusions of the PDF in the OCP the MPC is called stochastic MPC (SMPC). SMPC exploits the characteristics of the PDF to define chance constraints, which require the constraint to hold with some specific probability level [5] [13] [21] [22] [31]. Therefore enables SMPC for a systematic approach of finding a trade-off between constraint violations and conservative control actions. In the text below it is explained how to formulate a stochastic optimal control problem (SOCP).

For the formulation of the SOCP let us start with the OCP given by Equation (2.7). First, include some form of uncertainty in the OCP and formulate the constraints with uncertainty as chance-constraints. Examining the OCP that the variable bounds are the only inequality constraints, as the other constraints are the model equation. Therefore is all of the chance-constraint linear which was it usually in control [5] [13] [21] [31]. Before formulating the complete SOCP lets first look at how an individual chance-constraint is formulated. The general formulation of a chance constraint is given as:

$$\mathbb{P}\left(H^T y(\xi) \leq c\right) \geq \alpha. \tag{2.8}$$

In the above equation, $\mathbb{P}$ is the probability of holding the constraint, H^T is the constraint vector, $y(\xi)$ is the random variable given by some probability distribution ξ, c is the lower

bound of the constraint and α is the probability level.

For the chance-constraint given in Equation (2.8) lets rewrite it, as it is not easily interpreted. Assume that α is larger than 0.5 and let the covariance of $y(\xi)$ be given by Equation (2.9) and the variance given by Equation (2.10).

$$Y = \mathbb{E}(y(\xi) - \bar{y})(y(\xi) - \bar{y})^T. \tag{2.9}$$

Here Y denotes the covariance matrix of $y(\xi)$ and $\bar{y}$ denotes the expected value of $y(\xi)$.

$$\sigma^2 = H^T \mathbb{E}(y(\xi) - \bar{y})(y(\xi) - \bar{y})^T H = H^T Y H, \tag{2.10}$$

where σ is standard variance of $y(\xi)$.

Thereafter let us normalize the probability distribution such that the computations becomes easier.

$$p_n(\xi) = \frac{H^T y(\xi) - \bar{y}}{\sigma}. \tag{2.11}$$

In the above equation the probability distribution have been normalized, where $p_n(\xi)$ is the normal Gaussian distribution with unit variance and zero mean. Thereby by reformulating the linear constraint as:

$$h^T y(\xi) \leq c \Rightarrow \frac{H^T y(\xi) - \bar{y}}{\sigma} \leq \frac{c - \bar{y}}{\sigma} \Rightarrow p_n(\xi) \leq \frac{c - \bar{y}}{\sigma}. \tag{2.12}$$

Thereby using the above reformulation to rewrite the chance-constraint given by Equation (2.8), the constraint can be written as:

$$F_G\left(\frac{c - \bar{y}}{\sigma}\right) \geq \alpha. \tag{2.13}$$

Where F_G is the standard one dimensional Gaussian distribution function.

Then take the cumulative Gaussian distribution of Equation (2.13) the constraint can be written as:

$$\frac{c - \bar{y}}{\sigma} \geq F_G^{-1}(\alpha). \tag{2.14}$$

Where $F_G^{-1}(\alpha)$ is the inverse cumulative Gaussian distribution function of α.

Lastly let us shuffle the terms such that c get one side of the inequality and use Equation (2.10) for replacing the variance.

$$H^T \bar{y} + F_G^{-1}(\alpha)\sqrt{H^T Y H} \leq c \tag{2.15}$$

Then the chance-constraint in Equation (2.8) have been rewritten to something more easily interpreted.

Now that the individual chance-constraint have been formulated, one can go back to the OCP and look at how the constraint given by Equation (2.15) can included in the dynamic optimization problem given by Equation (2.7). As the problem is dynamic, it means that for each time period a chance-constraint needs to be added. Furthermore, if the constraint is an greater or equal constraint the same derivation as above can be used, just that one subtract the back-off. Therefore lets apply the chance constraint to the bounds on the variables in Equation (2.7), such that the SOCP can be formulated. In Equation (2.16) the stochastic optimal control problem is formulated.

$$\min_{\mathbf{U}} \quad \sum_{k=0}^{N-1} \mathbf{\Phi_k}\left(\mathbf{x_{k+1}}, \mathbf{z_{k+1}}, \mathbf{u_k}, \mathbf{p}, \xi\right) \Delta t_k \tag{2.16a}$$

$$s.t. \quad \mathbf{x_{k+1}} = \mathbf{f_k}\left(\mathbf{x_k}, \mathbf{z_k}, \mathbf{u_k}, \mathbf{p}, \xi\right), \quad \forall\, k = 1, .., N \tag{2.16b}$$

$$\mathbf{x_{k+1}}(0) = \mathbf{x_k}, \quad \mathbf{x_0}(t_k) = \text{given}, \quad \forall\, k = 0, .., N-1 \tag{2.16c}$$

$$\mathbf{g_k}\left(\mathbf{x_k}, \mathbf{z_k}, \mathbf{u_k}, \mathbf{p}, \xi\right) = 0, \quad \forall\, k = 0, .., N \tag{2.16d}$$

$$\bar{\mathbf{x}}_\mathbf{k} + F_G^{-1}(\alpha)\sqrt{\mathbf{X_k}} \leq \mathbf{x_{ub}}, \quad \forall\, k = 1, .., N \tag{2.16e}$$

$$\bar{\mathbf{x}}_\mathbf{k} - F_G^{-1}(\alpha)\sqrt{\mathbf{X_k}} \geq \mathbf{x_{lb}}, \quad \forall\, k = 1, .., N \tag{2.16f}$$

$$\bar{\mathbf{z}}_\mathbf{k} + F_G^{-1}(\alpha)\sqrt{\mathbf{Z_k}} \leq \mathbf{z_{ub}}, \quad \forall\, k = 1, .., N \tag{2.16g}$$

$$\bar{\mathbf{z}}_\mathbf{k} - F_G^{-1}(\alpha)\sqrt{\mathbf{Z_k}} \geq \mathbf{z_{lb}}, \quad \forall\, k = 1, .., N \tag{2.16h}$$

$$\mathbf{u_{lb}} \leq \mathbf{u_k} \leq \mathbf{u_{ub}}, \quad \forall\, k = 0, .., N-1 \tag{2.16i}$$

$$\tag{2.16j}$$

In the above equation, $\bar{\mathbf{x}}_\mathbf{k}$ is the expected value of $\mathbf{x_k}$, $\mathbf{X_k}$ is the covariance matrix of $\mathbf{x_k}$, $\bar{\mathbf{z}}_\mathbf{k}$ is the expected value of $\mathbf{z_k}$, $\mathbf{Z_k}$ is the covariance matrix of $\mathbf{z_k}$ and ξ is the uncertainty given by some probability distribution function.

Chapter 3

Model Description

The model that are described in this Chapter is based on a simplified version of the subsea installation for the Ormen Lange field. In the model the parameters describing the characteristics of the subsea separation system are taken from literature about the Ormen Lange field [8] [25] [35]. Some parameters are also adjusted so that the system fits operating conditions for the Ormen Lange field, these adjustments are given in Appendix B. In Figure 3.1 a diagram of the subsea system is shown. The system consist of the reservoir, a well-bore, vales, a gravity separator and a compressor. An explanation of how each unit is modelled is described in Sections 3.1-3.4.

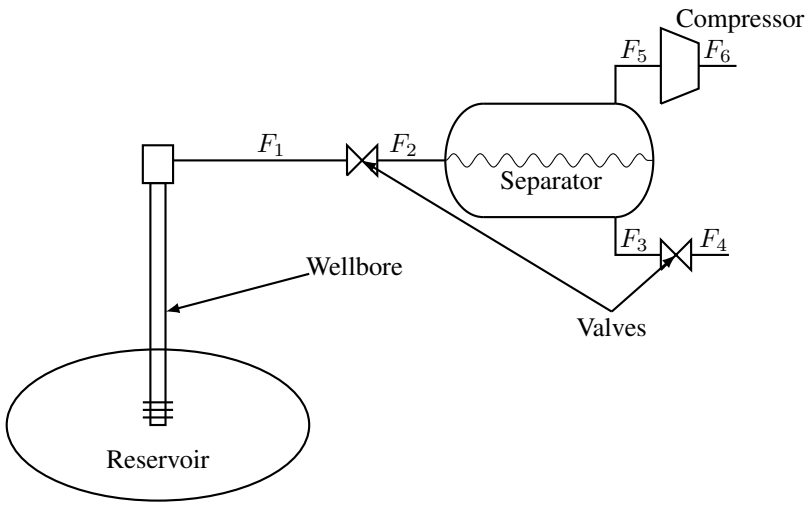

Figure 3.1: Diagram of the subsea separation system, consisting of the reservoir, well bore, valves, separator and compressor. Where the F_i indicates a stream i.

3.1 Reservoir

In this section the reservoir and well bore equations are derived and explained. With these equations one can find the well performance curves which is used to find the production of gas and oil. As the pressure gradient from the reservoir to the well bore is the main driving force of the system [18]. Given a pressure gradient the fluid in the reservoir will move towards the well bore-head, assuming that the pressure is lower at the well bore-head than in the reservoir. Darcy was the first to model how fluids moves through a solid in 1856 [43], whit the development of Darcy's law which is given in Equation (3.1). Even though Darcy found the relation between the pressure difference and flow rate through experiments it was later shown that it could be derived from Navier-Stokes law [43].

$$q_0 = J(P_r + P_{wf}), \tag{3.1}$$

where q_0 $\left[\mathrm{m^3\,s^{-1}}\right]$ is the flow rate, J $\left[\mathrm{m^3\,s^{-1}\,Pa^{-1}}\right]$ is the flow coefficient, P_r [Pa] is the average reservoir pressure and P_{wf} [Pa] is the well bore bottom hole pressure.

Darcy's Law gives a good estimation for unsaturated oil wells but not for saturated oil wells or gas wells [18] [41]. The reason for this is that Darcy's law assumes laminar flow and incompressibility of the fluid. These assumptions do not hold for gas wells or saturated oil wells. Vogel presented an empirical equation called Vogel Equation (3.2) in 1968 [41] after studying how the flow rate changes with the pressure gradient.

$$\frac{\dot{m}_o}{\dot{m}_{o_{max}}} = 1 - 0.2\left(\frac{P_{wf}}{P_r}\right) - 0.8\left(\frac{P_{wf}}{P_r}\right)^2. \tag{3.2}$$

Here $\dot{m}_o$ $\left[\mathrm{kg\,s^{-1}}\right]$ denotes the flow of oil and $\dot{m}_{o_{max}}$ $\left[\mathrm{kg\,s^{-1}}\right]$ denotes the maximum flow of oil, i.e. the flow when $P_{wf} = 0$.

Vogel equation (3.2) gives good results for saturated oil wells but not for high-velocity wells [18]. Fektovich also studied how the flow rate changed with pressure gradient [14]. Fetkovich did his study for gas and two-phase flows while Vogel had mainly done for oil wells [18]. Fektovich equation (3.3) showed good result both for gas and oil wells.

$$\dot{m}_i = k_i\left(P_r^2 - P_{wf}^2\right)^n, \tag{3.3}$$

where $\dot{m}_i$ $\left[\mathrm{kg\,s^{-1}}\right]$ is the flow of component i, k_i $\left[\mathrm{kg\,s^{-1}\,Pa^{-2n}}\right]$ is the flow coefficient for component i and n is deliverability exponent, where n is from 0.5 - 1.0.

In this work, the Fektovich Equation (3.3) will be used for the estimation of the oil and water flow rates. The reason for this is that the Ormen Lange is a gas reservoir and the Fektovich equation has shown best results for gas reservoirs. The gas-oil-ratio (GOR) is used, which is given by Equation (3.4). The gas flow is given by Equation (3.5)

$$GOR = \frac{k_g}{k_o}\left(P_r - P_{wf}\right)^2, \tag{3.4}$$

$$\dot{m}_g = \frac{k_g}{k_o}\dot{m}_o \left(P_r - P_{wf}\right)^2, \tag{3.5}$$

in the above equations k_g $\left[\mathrm{kg\,s^{-1}\,Pa^{-2n+2}}\right]$ is the flow coefficient for gas and k_o $\left[\mathrm{kg\,s^{-1}\,Pa^{-2n}}\right]$ is the flow coefficient for oil.

For the pressure drop from the reservoir to the seabed, the stationary mechanical energy balance is used. It is assumed that there is no slip between the phases, no friction and that work and kinetic energy can be neglected. Furthermore it is assumed that the fluid is a single-phase pseudo-fluid with negligible mixing volumes and density is given by the volume average of the fluid. Then the pressure drop is given by Equation (3.6).

$$dp = \rho_{mix} g dh, \tag{3.6}$$

where dp [Pa] is the pressure drop, ρ_{mix} is the density of the mixture given by Equation (3.7), g $\left[\mathrm{m\,s^{-2}}\right]$ is the gravitational constant and dh [m] is the height difference between the reservoir and seabed.

$$\rho_{mix} = \frac{\dot{m}_g + \dot{m}_o + \dot{m}_w}{\frac{\dot{m}_g}{\rho_g^{ig}} + \frac{\dot{m}_o}{\rho_o} + \frac{\dot{m}_w}{\rho_w}}. \tag{3.7}$$

In the above equation ρ_g^{ig} $\left[\mathrm{kg\,m^3}\right]$ denotes the density of gas assuming ideal gas law.

The pressure at the seabed is found by integrating Equation (3.6) from (P_{wf}, h_r) to (P_1, h_1) which gives:

$$\dot{m}_1 g \Delta h = \frac{\dot{m}_g R T_r}{M_g} \ln\left(\frac{P_1}{P_{wf}}\right) + \left(\frac{\dot{m}_o}{\rho_o} + \frac{\dot{m}_w}{\rho_w}\right)\left(P_{wf} - P_1\right) \tag{3.8}$$

Here R $\left[\mathrm{J\,K^{-1}\,mole^{-1}}\right]$ denotes the universal gas constant, T_r [K] denotes the temperature of the reservoir, M_g $\left[\mathrm{kg\,mole^{-1}}\right]$ denotes the molar weight of the gas and P_1 [Pa] denotes the pressure at the seabed.

The logarithmic term in Equation (3.8) can be simplified with using Taylor series. This is shown in Equation (3.9).

$$\ln\left(\frac{P_1}{P_{wf}}\right) = \ln\left(\frac{P_{wf}}{P_{wf}} + \frac{P_1 - P_{wf}}{P_{wf}}\right) = \ln\left(1 + \frac{P_1 - P_{wf}}{P_{wf}}\right) \approx \frac{P_1 - P_{wf}}{P_{wf}} \tag{3.9}$$

Inserting Equation (3.9) into Equation (3.8) one can express P_1 as a function of P_{wf}. The result is given in Equation (3.10).

$$P_1 = P_{wf} + \frac{\dot{m}_1 g P_{wf} \Delta h}{\frac{\dot{m}_g R T_r}{M_g} + P_{wf}\left(\frac{\dot{m}_o}{\rho_o} + \frac{\dot{m}_w}{\rho_w}\right)} \tag{3.10}$$

Assuming that there are no accumulation of mass in the well bore, therefore due to the conservation of mass the mass flow into the well bore is the same the mass flow out.

Furthermore one also assumes that the system are in equilibrium so the mass fraction is also constant over the well bore.

Reservoir degeneration

The pressure inside a reservoir will decrease over the lifetime of the reservoir. The pressure decrease are caused by gas and oil being pumped out of the reservoir. There exist many different models for modelling how the pressure decreases. These models can based in physical and/or historical data [18]. In this Master thesis an empirical model is used and is given by Equation (3.11). This model assumes that the pressure decrease is linear with respect to time. This model is used as overall pressure decrease data for the Ormen Lange field was not available.

$$\frac{dP_r}{dt} = C, \qquad C < 0, \tag{3.11}$$

here C $\left[\mathrm{Pa\,s^{-1}}\right]$ stands for the reservoir degeneration factor.

3.2 Valves

Valves are often included into a system for control. By adjusting the position of the valve-head one can increase/decrease the pressure drop over the valve, which can be used for controlling the flow. The valve equation from [33] is used for modelling the flow through a valve and is given by Equation (3.12).

$$\dot{m} = C_v f(y) \sqrt{\frac{\Delta P}{SG}}, \tag{3.12}$$

where C_v $\left[\mathrm{kg\,s^{-1}\,Pa^{-1/2}}\right]$ is the valve coefficient, $f(y)$ is the valve characteristic function dependent on the position of the valve-head, z, ΔP [Pa] is the pressure drop over the valve and SG is the specific gravity of the fluid.

The valve characteristic function indicates how the flow changes with the position of the valve-head, y. If y is equal to one it indicates fully open valve and if y is equal to zero that the valve is closed. In this Master thesis lets assumes that the valve characteristics function is linear with respect to y, which is shown in Equation (3.13).

$$f(y) = y. \tag{3.13}$$

In the above equation y is the position of the valve-head and where y takes values from zero to one.
Furthermore one assumes that the system is in equilibrium over the valve so the mass flow and mass fractions are consistent over the valve.

3.3 Separator

In this section the separator model is derived and explained. The separator is used for separating the different phases of the fluid; gas and liquid. For this separation a horizontal gravity separator is used. The dynamics of the separator are very depending on the design of the separator, where different inlet diverter, internal vessels etcetera will change the dynamics of the separator [2] [23] [36] [37]. The separator can be divided into three major parts; inlet, gravity section and demister [2]. A figure of a three phase gravity separator is shown in Figure 3.2, where the three major parts are indicated. At the inlet the stream will hit the inlet diverter and have a change of momentum. This change of momentum will separate the liquid and gas. The inlet diverter is also used for distribution of the gas. The design of the inlet diverter will dictate what kind of distribution occurs [23]. Gravitational forces will separate the different components depending on the density of the components, this is the main separation process in the gravity section. In the liquid phase, gas bubbles will rise due having lower density than the liquid and similarly, for liquid droplets in the gas phase. In the gravity settling section one can also have internal vessels like mesh pads and vane packs to enhance the separation of gas and liquid [23]. Before the gas leaves the separator, it will go through a demister. The demister will separate out some of the remaining droplets in the gas phase. The demister can have different designs [36] and what kind of separation process that occurs is dependent on the design. The design of the demister also effects the effectiveness of the droplet removal [36], where some demister can effectively remove droplets down to the size of 3-5 $\mu\,\mathrm{m}$ [23]. In this work the inlet diverter and demister are not included in the modelling. Therefore the separator model only consist of the gravity section.

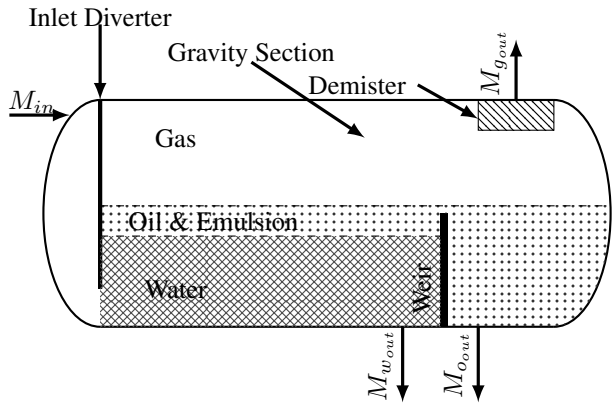

Figure 3.2: Schematic of a horizontal three-phase gravity separator, with the three major separation parts; Inlet, gravity settling and demister.

Assuming that no mass is accumulated inside the separator, the overall mass balance is:

$$\dot{m}_{in} = \dot{m}_{g_{out}} + \dot{m}_{l_{out}} \tag{3.14}$$

In Equation (3.14) if one assumes that the flow into the separator is known, then there are

two unknowns and one equation. Therefore another equation is needed for solving both of the outlet flows. Figure 3.3 shows a basic overview of the in and out flows along with the internal flows.The two internal flows, F_g and F_l, are the flows of gas from the liquid phase to the gas phase and the flow of liquid from the gas phase to the liquid phase, respectively. Assuming that the mass fractions at the inlet is known, the component mass balances can be solved. For modelling liquid in gas or gas in liquid, one can use multiphase flow theory [9]. For this Master thesis multiphase flow theory is not used because of the complexity. Instead, a simplified expression is used to describe the amount of liquid that leaves with the gas and the amount of gas leaving with the liquid.

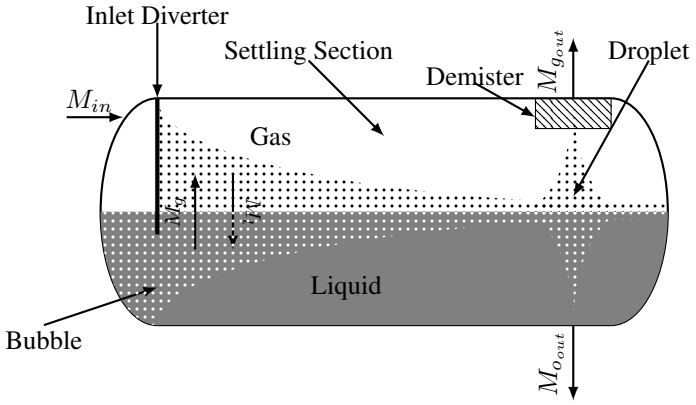

Figure 3.3: Show the separation of droplets from the gas phase and bubbles from the liquid phase for a gravity separator.

The amount of liquid that goes out with the gas is called the liquid carryover and the gas leaving with liquid is called the gas carryunder. In the section below only the how the modelling of liquid carryover is discussed, but similiar equations can be used to model the gas carryunder.

Let the droplet velocity towards the interface be govern only by the size of the droplet and gas properties. This assumption implies that the droplets have constant density, there is no break-up or coalescence, no re-entering of droplets from the liquid phase into the gas phase. Additionally, that the separation is isothermal and the droplets size is independent of the vertical position. Finally assume that the size of the droplets is determined by the design of the separator and the inlet conditions and that the separation coefficient is constant. With these assumptions and simplifications one can express the liquid carryover as a function of the residence time and the separation coefficient. The expression of the is given in Equation (3.15). The expression is taken from [38], and the expression is not very accurate, due to the number of assumptions and simplifications made. But nonetheless it is used in this Master thesis as an indication of liquid carryover.

$$\frac{dZ_o}{d\tau} = -S_o\tau, \tag{3.15}$$

where τ [s] is the residence time and S_o $\left[\mathrm{s}^{-2}\right]$ is the separation efficiency for the oil.

When solving Equation (3.15), the mass fraction of gas/liquid can be found for the two outlet streams. The mass fraction is given by Equation (3.16).

$$Z_{5,o} = \frac{\dot{m}_{in}}{\dot{m}_j} Z_{2,o} \exp\left(-S_o \frac{V_g}{\frac{\dot{m}_5}{\rho_5}}\right). \tag{3.16}$$

In the equation above Z_{5_o} is the mass fraction of oil in outlet stream 5, see Figure 3.1, V_g $\left[\mathrm{m}^3\right]$ is the volume of the gas phase in the separator given by Equation (3.17), $\dot{m}_5$ $\left[\mathrm{kg\,s}^{-1}\right]$ is the mass flow in stream 5, and ρ_5 is the density of outlet stream 5 and it is given by Equation (3.18).

$$V_g = V_{sep} - L((h-R)\sqrt{2Rh-h^2} + R^2 \arccos\left(1.0 - \frac{h}{R}\right), \tag{3.17}$$

where V_{sep} $\left[\mathrm{m}^3\right]$ is whole volume of the separator, L [m] is the length of the separator and R [m] is the radius of the separator.

$$\rho_5 = \rho_w \left(Z_{5,g} SG_g + Z_{5,o} SG_o + Z_{5,w} SG_w\right). \tag{3.18}$$

For the equation above ρ_w $\left[\mathrm{kg\,m}^{-3}\right]$ is the density of water, SG_g $[-]$ is the specific density of the gas, SG_o $[-]$ is the specific density of the oil and SG_w $[-]$ is the specific density of water.

For finding the liquid in stream 5 the component balances for the separator can be used. The component balance are given as:

$$Z_{2,o}\dot{m}_2 = Z_{5,o}\dot{m}_5 + Z_{3,o}\dot{m}_3 \tag{3.19}$$

By combining Equations (3.14), (3.16) and (3.19) the mass flows out and the separator, along with the corresponding mass fraction, can be expressed..

The components are in this work considered to be; gas, oil and water. Also it is assumed that there are no water in stream 5 as water have a higher density than oil.

3.4 Compressor

The compressor is used to increase the pressure of the gas outlet stream such that the pressure is high enough to transport itself to the top-side processing plant.

The stream entering the compressor is assumed to be only gas, then the static-head terms, velocity-head terms and friction terms can be neglected [16]. The mechanical energy balance for compression of gas is given in Equation (3.20).

$$dWs = \frac{dP}{\rho}, \tag{3.20}$$

where $dWs\ \left[\mathrm{J\,kg^{-1}}\right]$ is the specific work done by the compressor, dP [Pa] is the pressure increase over the compressor.

The compression is assumed to be adiabatic. Therefore that the compression follows an isentropic path way, which is given by Equation (3.21).

$$\frac{P}{P1} = \left(\frac{\rho_1}{\rho}\right)^{\gamma} \tag{3.21}$$

Equation (3.21) is inserted into Equation (3.20) and then integrated from (W_0, P_1) to (W, P_2) then solve for W. Assuming ideal gas law holds, the adabatic compression work canb e expressed as:

$$W_s = \frac{\gamma}{\gamma - 1}\frac{RT_1}{M}\left(\left(\frac{P2}{P1}\right)^{\left(\frac{\gamma-1}{\gamma}\right)} - 1\right), \tag{3.22}$$

here $W_s\ \left[\mathrm{J\,kg^{-1}}\right]$ denotes the specific work done by the compressor and γ denotes the heat capacity ratio.

The total work of the compressor, the specific work defined in Equation (3.22) is multiplied with the mass flow and divided by the compressor efficiency, this is shown in Equation (3.23).

$$W = \frac{\gamma}{\gamma - 1}\frac{RT_1}{M}\left(\left(\frac{P2}{P1}\right)^{\left(\frac{\gamma-1}{\gamma}\right)} - 1\right)\left(\frac{\dot{m}}{\eta}\right), \tag{3.23}$$

Where η is the compressor efficiency.

Compressor Degeneration

As times goes, the compressor efficiency will decrease and the probability of breakdown of the compressor will increase. The reason for this is mainly wear and tear of the compressor. An empirical mode is used to model the decrease of compressor efficiency. No statistical or physical models for such degradation are available, therefore a simple linear model is used. For the probability of breakdown it is assumed that it is correlated with the compressor efficiency. Therefore no model of the breakdown is presented in this work. For the degeneration of compressor efficiency it is given by Equation (3.24). Where it is assumed that liquids will have a higher wear and tear factor than gas on the compressor, as the compressor is designed for handling gas, not liquids.

$$\frac{d\eta}{dt} = A\dot{m}_g + B\dot{m}_l. \tag{3.24}$$

In the above equation, A $\left[\mathrm{kg^{-1}}\right]$ is the gas degeneration factor and B $\left[\mathrm{kg^{-1}}\right]$ is the liquid degeneration factor, with $0 > A > B$.

Chapter 4

Optimal Control Problem Formulation

In this chapter the optimal control problem (OCP) for the subsea separator system described in Sections 3.1-3.4 is explained. Where each of the three majors part of the OCP is discussed. First a degree of freedom analysis is done, this is for deciding the control variables

4.1 Degree of Freedom Analysis

The subsea separation system is considered to be controlled by a model predictive controller (MPC). The MPC is controlling the system by adjusting some variable such that the some variables are kept at desired values. The variables that are adjusted is called manipulated variables (MVs), while the variables that are kept at the desired values is called control variables (CVs) [33]. For the subsea separation system these CVs can be found from analysing the set of model equations given in Sections 3.1-3.4. From analysing the model equation one finds that there are 3 more variables than equations, therefore there are 3 degree of freedom for control. The CVs that was chosen is: separator pressure, P_2, liquid height in the separator, h, and the compressor duty, W. The reservoir pressure can be used for controlling the pressure drop between the reservoir and well bore-head, thereby controlling the mass flow. The liquid height in the separator can control the mass fractions in the gas outlet and the liquid outlet of the separator by changing the residence time of the liquid and gas, see Equations (3.16) and (3.17). The last CV is the compressor duty as it can control the pressure in stream 6, see Equation (3.23).

4.2 Optimal Control Problem

The OCP for the subsea separation system will have a same formulation as the ones used in Chapter 2. So the formulation used in Equation 2.7 will be used when there is no uncertainty in the system, while Equation 2.16 will be used when there is uncertainty in the system. The objective function, constraint and variables bound is explained below.

4.2.1 Objective Function

From Equation 2.7 the objective function is given as :

$$\sum_{k=0}^{N-1} \mathbf{\Phi_k}\left(\mathbf{x_{k+1}}, \mathbf{z_{k+1}}, \mathbf{u_k}, \mathbf{p}\right) \Delta t_k \tag{4.1}$$

If the system had some uncertainty the objective function from Equation 2.16 was used, and is given as:

$$\sum_{k=0}^{N-1} \mathbf{\Phi_k}\left(\mathbf{x_{k+1}}, \mathbf{z_{k+1}}, \mathbf{u_k}, \mathbf{p}, \xi\right) \Delta t_k \tag{4.2}$$

From the two above equations $\mathbf{\Phi_k}$ is the scalar function which describes the properties of the system that one want to minimize or maximize. For the subsea separation system this property is the profit, as higher profit would make the system operate more efficiently.

The subsea separation system model in this work is a simplified version of the Ormen Lange subsea installation. The Ormen Lange field consist mostly of gas [35] [40], therefore is the production of gas much larger than the production of oil. Assuming that the income from the oil production can be neglected, the income is given by the amount of gas produced. For the expenses assume that they are not affected by the production volume of the system and therefore fixed values. As the expenses are fixed values they can be removed from the OCP without effecting the optimal solution. With these assumptions the maximizing of the profit is the same as maximizing gas production. In Equation (4.3) an objective function that maximize gas production is presented.

$$\sum_{k=0}^{N-1} p_k \dot{m}_{6_{k+1}} Z_{6,g_{k+1}} \Delta t_k, \tag{4.3}$$

where N is the number of time periods, p_k is the price of gas in time period k, $\dot{m}_{6_{k+1}}$ $\left[\mathrm{kt\,d^{-1}}\right]$ is the mass flow in stream 6, see Figure 3.1, for time period k, $Z_{6,g_{k+1}}$ $[-]$ is the mass fraction of gas in 6 for time period k and Δt_k [d] is the length of time period k.

4.2.2 Constraints

The constraints are functions that restricts the feasible region of the optimization problem. For the OCP of the subsea separation system the feasible region one are interested in are

where the model equations hold. By adding the model equations from Sections 3.1-3.4 as constraints, the feasible region would be restricted to where the model equations holds. In Equations 2.7 and 2.16 the constraint was divided in three. These three set of constraint was the differential equations, algebraic equations and continuity constraints. In the model equations there are two differential equations, Equation (3.11) and (3.24), while the rest is algebraic. Furthermore, as the time horizon is divided into N time steps, one has to add all of the model equations as constraints in each time period. Therefore the number of constraints is the number of model equations multiplied with the number of time steps. The last set of constraints is the continuity constraints, these connect time period k with $k+1$. For connecting the two time periods with each other the end time value of period k need to be found. For finding the values at the end of a time period there exist a large variety of methods, in this work collocations was used.

4.2.3 Upper and Lower Bounds

The upper and lower bounds restrict the values of the states. In Table A.2 all of the upper and lower bounds is given. The bounds are given by physically restriction on the states ,system design restrictions and engineering insight of the system. Some of the bounds that are chosen by the insight into the system will be explained in more details here. The upper bounds on the mass fraction of gas in stream 3 and oil in stream 5 is chosen such that gas carryunder and liquid carryover is kept below those bounds. With restricting the gas carryunder and liquid carryover the solutions with poor separation efficiency is removed. The lower bound of the pressure in stream 6 is given such that the pressure is sufficient to drive the gas from the subsea installation to the topside receiving facility. Lastly the lower bound of compressor duty is given as an indication for when the compressor need maintenance.

4.2.4 Chance-Constraint

Chance-constraints was added to the OCP for handling uncertainty in the system. Chance-constraint was chosen as it gave a trade-off between number of constraint violations and how large the back-off from the optimal conditions is. In Section 2.2 the chance-constraint was given as:

$$h^T \bar{y} + F_G^{-1}(\alpha)\sqrt{h^T Y h} \leq g. \tag{4.4}$$

For being able to formulate the chance-constraint in Equation (4.4) the expected value of the variable, $\bar{y}$, the inverse cumulative Gaussian distribution function, $F_G^{-1}(\alpha)$, and the covariance matrix, Y needs to be found. These variable can be found by the probability distribution function (PDF) of y, where y stands for the differential or algebraic variables. The PDF of y can be approximated by doing Monte Carlo simulations [10] [15], assuming that the uncertainty in the system can be expressed by some known PDF. Monte Carlo simulation work with one simulates the system multiple times with random outcomes of the uncertainty. Then the PDF of y can be approximated from the results of the simulations. For more about Monte Carlo simulations see *Monte Carlo: Concepts, Algorithms,*

and Applications [15].

Chapter 5

Case Studies

For studying the OCP described in Chapter 4 four different cases have been studied. These cases have been chosen to get an understanding of the system by stepwise include additional terms to the objective function. These cases are also to illustrate how changes in the OCP can change the solution and how this can cause constraint violations and sub-optimal operating conditions. In Section 5.1 the first case where the time horizon is fixed is presented. In Section 5.2 the time horizon is added as an additional degree of freedom, which is case 2. Thereafter, in 5.3 the third case is presented, where present value is included in the objective function. Lastly, in Section 5.4 uncertainty is included in the system.

5.1 Case 1: Fixed Time Horizon

The time horizon of the OCP is given by when the maintenance of the compressor occur. Assuming a fixed time horizon for the OCP because the compressor maintenance is scheduled for given time in the future. That the maintenance is performed after a given time period can be because it is company policy, the guarantee on the equipment expires or special equipment are need to perform the maintenance.

In case 1 the time horizon is fixed, so by dividing the time period into equally large sections the length of the time period, Δt_k, can be removed from the objective function without effecting the optimal solution. Furthermore, in case 1 it is assumed that the price of the gas is constant throughout the time horizon, and can therefore also be removed form the objective function. With these assumption the objective function is given as:

$$\sum_{k=0}^{N-1} \dot{m}_{6_{k+1}} Z_{6,g_{k+1}}. \tag{5.1}$$

Case 1 is studied for getting an insight into how the system behaves and what the optimal conditions of the system is.

5.2 Case 2: Varying Time Horizon

In case 1 the time horizon was fixed as it was assumed that the maintenance was scheduling for given time in the future. If the time period is short to would lead to unnecessary maintenance. Since the equipment is at the seabed the expenses associated with maintenance is large. Therefore if the maintenance is occurring too regularly it will it will lead to large maintenance expenses over time. If the time period is to long it could lead to failure in the equipment. As the equipment is not easily accessible for repair, the time before repair can be done is large. This will lead to large time periods of down time which causes loss in income. Furthermore, one also want to prevent failures, such that accident like the *"Deepwater Horizon"* accident do not occur. So for scheduling maintenance of the compressor it should not be too often or too infrequently. For planning the optimal time for preforming the maintenance the time for maintenance is added to the OCP, such that the end time becomes a variable.

In case 2 one still assumes that the price of gas is constant throughout the time horizon, and can therefore be removed from the objective function. But since the end time is variable the length of the time periods can no longer be removed from the objective function. Assume that all of the time periods is divided such that they are equally large. With these assumptions the objective function for case 2 is:

$$\sum_{k=0}^{N-1} \dot{m}_{6_{k+1}} Z_{6,g_{k+1}} \Delta t_k. \tag{5.2}$$

For preventing the end time to be negative or be unrealistic large, variables bounds on the end time need to be added. These bounds are given in Table A.1. For the differential, algebraic and control variable the bounds was added for each time period, this is not needed for the end time as it is consistent in all time periods. Therefore is it enough to add just one extra lower and upper bound for the end time.

Case 2 is studied to examine how addition of end time as a degree of freedom changes the optimal solution. Moreover, it is discussed why the reason for the change in the optimal solution can be.

5.3 Case 3:Net Present Value

In the two cases above the price of gas is assumed constant over the time horizon. Even if the price of gas is constant over the the time horizon it does not mean that the value of the income from the gas is constant over the time period. This is because income today can be used for other investments or be set in a bank account an earn interest. For calculating income in different times in the future net present value (NPV) is used. The calculation of NPV is given by Equation (5.3).

$$PV = \frac{C_f}{(1+i)^n}, \tag{5.3}$$

where PV is the net present value, C_f is the income, i is the interest rate and n is the number of time periods from the present the income occur.

For case 3 the NPV is included in the objective function, this is to examine if different prices of the gas have an effect on the optimal solution. With the inclusion of NPV in the objective function the objective function will be given as:

$$\sum_{k=0}^{N-1} \frac{C}{(1+i)^k} \dot{m}_{6_{k+1}} Z_{6,g_{k+1}} \Delta t_k. \tag{5.4}$$

In case 3 it is studied how the optimal control sequence changes when there is different prices on the gas. Moreover, the reasons for why the optimal solution changes when NPV is considered are discussed.

5.4 Case 4: Uncertainty

For the subsea separation system described in Sections 3.1-3.4 there can be many sources of uncertainty. In this work it is assumed that the uncertainty comes from model mismatch, this is because all of the assumptions and simplifications done in the modelling. In the model there is a number of parameters that was adjusted such that the system fitted operating data for the Ormen Lange field, see Appendix B. Since these parameters are adjusted from the steady-state condition of the Ormen Lange field there is no certainty that it holds when the operating conditions are changed. Therefore will these parameters considered as the main source of uncertainty for the system. In this case it assumed that uncertainty lies in the reservoir flow coefficient for oil, k_o.

Because of uncertainty a back-off from the constraint is usually added such that the probability of constraint violation is kept above some safety margin. In this work the back-off is calculated by use of chance-constraint. For calculating the back-off with use of chance-constraint the probability distribution function (PDF) of the variables need to known. The PDF of the variables can be approximated with use of Monte Carlo simulations, if the PDF of the uncertainty is known. Therefore it is assumed that the PDF of k_o is Gaussian distribution function with mean value of 0.016 and a variance of 0.0016.

For some constraint the probability of constraint violation is below the safety margin without adding a back-off. The reason for this can be that the state is far away from the constraint or the state is not effected by the uncertainty. For finding the constraints they may be violated, the deterministic problem is solved first. Therefore by examining the results from the previous cases the constraints that are active can be identified. Monte Carlo simulations are then performed such that the PDFs can be found for the active constraints. The PDFs are examined to see how the uncertainty effects the different active constraints. Examining how the uncertainty is effecting the probability of constraint violation the probability level can be decided. The probability level decides the probability that the constraints are violated. The probability levels are often given by safety margins of the equipment. In this

work it is assumed that the probability level is 0.95.

With the PDF and probability level the chance-constraints can be calculated. The back-off calculated by the chance-constraint is added and the OCP is solved. Since back-offs are added to the active constraints the solution of the OCP will change. With new solution the state of the system is changed. This can cause the system to behave differently such that new constraint becomes active or that the PDFs is changed. With different active constraint back-off may be needed to reduce the probability of constraint violation for these constraint also. If the PDF is changed it means that back-off calculate by the chance-constraint may be too large/small. Therefore is new Monte Carlo simulation performed such that back-off calculated by the chance-constraint have a probability of constraint violation equal to the probability level. Then the OCP is solved again. This is done in an iterative process until number of constraints violations are the same as the probability level plus/minus some error. Furthermore, with end time as a variable the iterative process start to oscillate. Therefore is the end time not included as a variable in case 4, instead the end time from case 3 is used.

Chapter 6

Results and Discussion

In this chapter the results from the optimization for the 4 cases described in Chapter 5 are presented and discussed. In Section 6.1 the results from case 1 is presented and discussed. The results from case 2 is presented in Section 6.2. In Section 6.3 the results from the optimization of case 3 is presented and discussed. Then in Section 6.4 the results from the optimization with uncertainty are presented and discussed.

All calculations were done in Python 2.7. The optimal control problem was formulated in CasADi 3.0 [1]. The optimization solver used was Ipopt 3.12.3. The python scripts can be found in Appendix D and the parameters, initial values and variables bounds used in the calculations can be found in Appendix B.

6.1 Results Case 1: Fixed Time Horizon

In this section the results for case 1 are presented. It is discussed how the control sequence is optimizing the gas production for the subsea separation system described in Sections 3.1-3.4. Furthermore, the active constraints are discussed along with how they are effecting the control sequences.

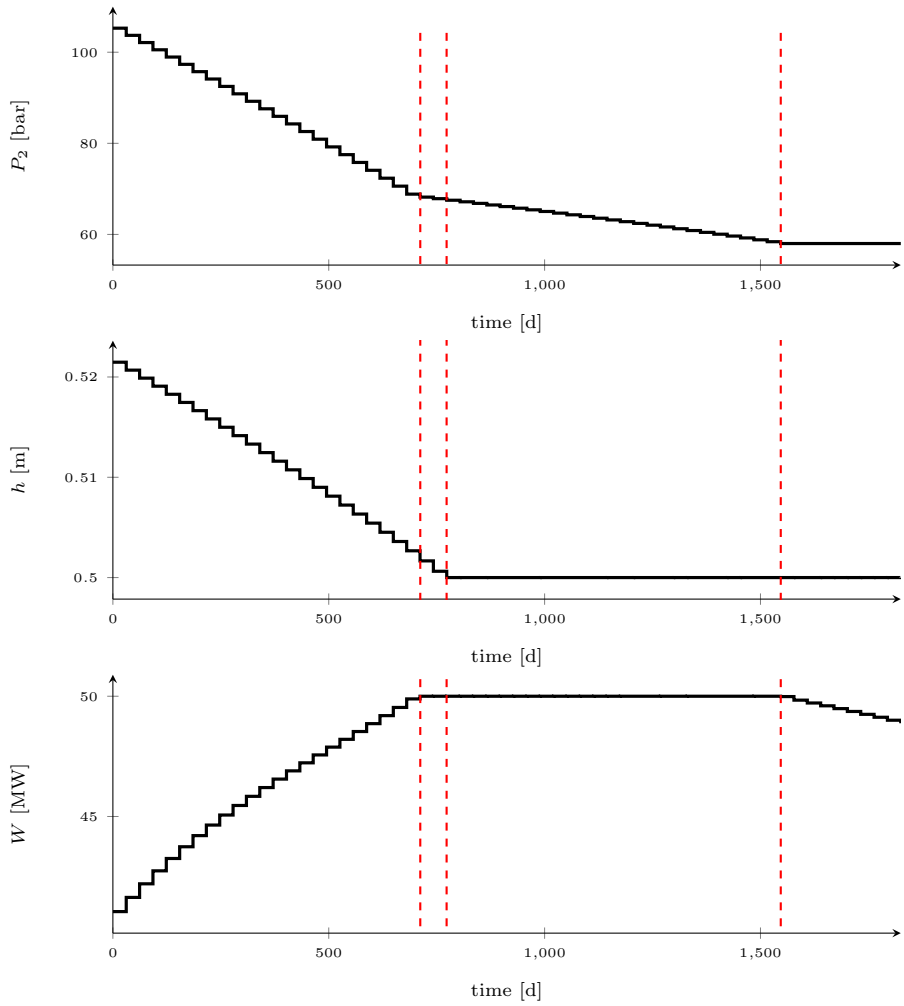

Figure 6.1: The optimal control sequences for the fixed time horizon optimization. Where P_2 [bar] is the pressure in the separator, h [m] is the liquid level in the separator and W [MW] is the compressor duty.

In the figure above the optimal control sequence for case 1 is given. In the figure there are three dotted lines, the first dotted line indicates when the upper bound on the compressor duty is reached. The second line indicates when the lower bound on the liquid height in the separator is reached, and the last line indicates when the lower bound on the separator pressure is reached.

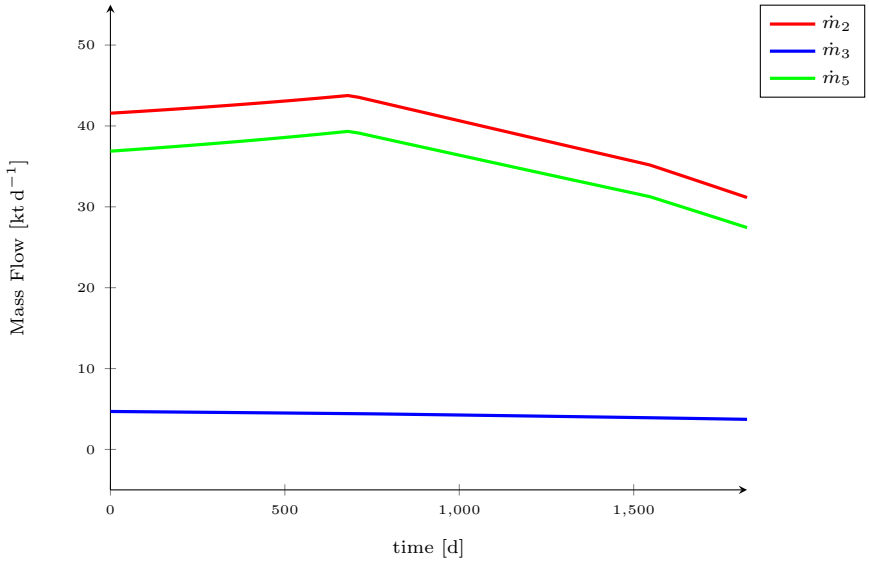

Figure 6.2: The mass flows in and out of the separator, see Figure 3.1, for the optimization with fixed time horizon.

From Section 5.1 the objective function of case 1 was to maximize gas production. In Figure 6.2 the mass flows of stream 2, 3 and 5 are given, which are the flows in and out the separator, see Figure 3.1. From the graphs one can see that the flows never reaches the upper bound for the mass flows which is 45.34 $\left[\mathrm{kt\,d^{-1}}\right]$. Therefore must there be a bound that restricts the mass flow for increase, thereby increasing the gas production. In Section 4.1 a degree of freedom analysis was done for the subsea separation system. From that analysis it was found that the separator pressure was determines the mass flows. From Figure 6.1 the separator pressure is not at the lower bound before the end of the time horizon. The separator pressure only restricts the mass flow from increasing at the end of the time horizon, so there must be another bounds that restricts the mass flows before that. From the plot of the compressor efficiency, see Figure 6.3, the lower bound is reached at the end of the time horizon. From Equation (3.24) the degeneration of the compressor efficiency is given by the mass flow into the compressor. If one was to increase the mass flows the mass flow into the compressor would also increased. This would caused compressor efficiency to drop below its lower bound. So the optimizer finds the maximum gas production that does not decrease the compressor efficiency below its lower bound.

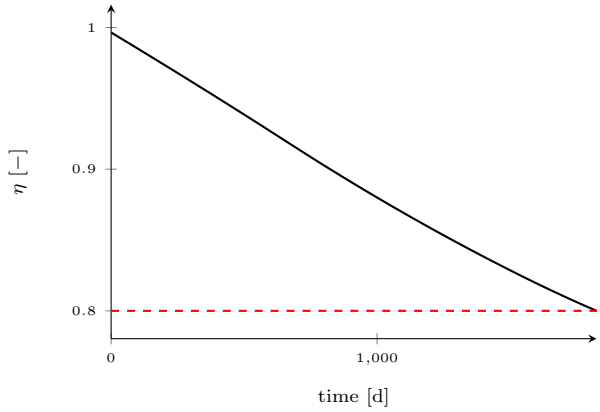

Figure 6.3: The compressor efficiency, η, for the optimizing with fixed time horizon.

From Equation (3.24) there are two terms to the degeneration of the compressor efficiency, one for the gas mass flow and one for the oil mass flow. From Table A.1 the gas damaging factor, A, is -3.0×10^{-6} [kg^{-1}] while the oil damaging factor, B, is -3.0×10^{-5} [kg^{-1}]. Comparing those two parameters, that the oil damaging factor is 10 times larger than the gas damaging factor. So if the mass fraction of oil in stream 5 was to decrease the production of gas could increase. From the degree of freedom analysis the liquid height in the separator was chosen for controlling the mass fractions. The mass fraction is given by the residence time and separation efficiency which is a constant. For the residence time for the oil in the gas phase, it is given by volume of the gas phase and the volumetric flow of stream 5. Thereby increasing the volume of the gas phase would increase the residence time of the liquid in gas, thereby decreasing the mass fraction of oil in stream 5. The volume of the gas phase is changing inversely with the liquid height of the separator, so if the liquid height is at the minimum one would get the best separation of oil as possible. From Figure 6.1 the liquid height in the separator is not at the lower bound in the beginning. Therefore must there be a bound that restricts liquid height. In Figure 6.4 the mass fraction of gas in stream 3 is presented. From the plot one can see that mass fraction of gas in stream 3 is at its upper bound in the beginning. Earlier it was stated by decreasing the liquid height the mass fraction of oil in stream 5 will decrease. If the liquid level is decreased it would mean that the residence time of the gas in the liquid would increase. Thereby would the separation efficiency of the gas decrease, meaning that the mass fraction of gas in stream 3 would increase. So the restriction on the liquid level is that the mass fraction of gas for stream 3 as its upper level. Therefore in the beginning it is the upper bound on the mass fraction of gas in stream 3 that restricts the separation of oil from the gas phase.

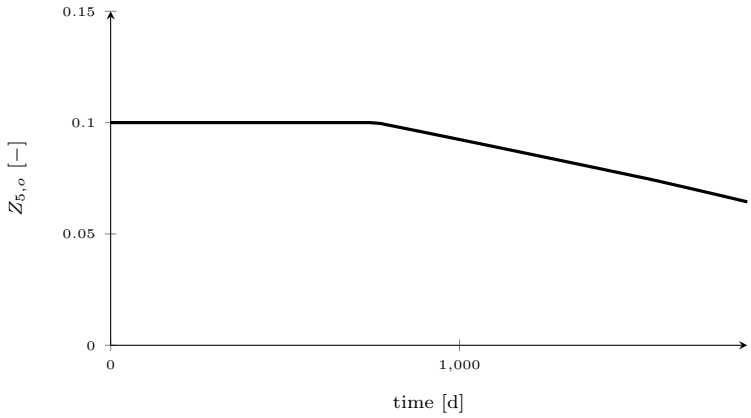

Figure 6.4: The mass fraction of gas in stream 3, for the fixed time optimization.

From Figure 6.2 two bends in the mass flow for stream 2 and 5. Comparing when the bends occur with when the compressor duty reach its upper bound, see Figure 6.1, that the first bend occur at the same time. Therefore it seems that this first bend in the mass flow is because of the compressor duty is at the upper bound. In Equation (3.23) the expression for the compressor duty is given. From that equation that the compressor duty is given by the pressure increase over the compressor, mass flow and the compressor efficiency. Form Figure 6.1 that the compressor duty is kept at its upper bound and from Figure 6.2 that the mass flow is decreasing. Therefore it means that the pressure increase over the compressor need to increase or the compressor efficiency is decreasing. From Figure 6.5 and Figure 6.1 that the pressure in stream 6 is at the lower bound when the compressor duty is at its upper bound. This was expected, as the degree freedom analysis that the compressor duty was used for controlling the pressure in stream 6. Looking at Figure 6.1 again that the pressure in the separator is decreasing, this means the pressure increase over the compressor is increasing. So the pressure increase over the compressor is the cause of the decrease in mass flow. But examining Equation (3.24) that the compressor efficiency will also decrease. Therefore is the decrease of mass flow not only cause by an increase in the pressure over the compressor but also from a decrease in compressor efficiency.

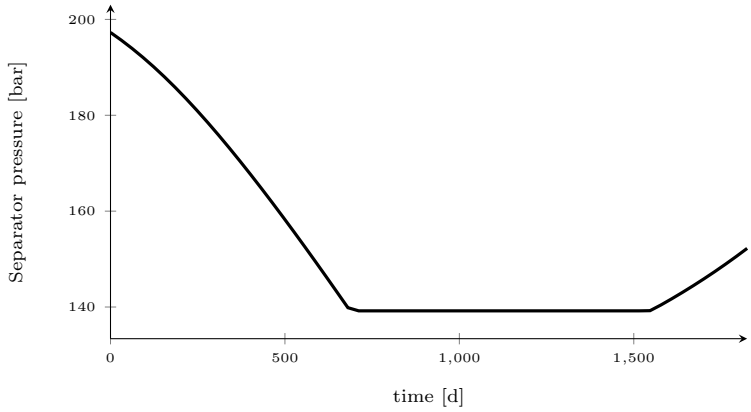

Figure 6.5: How the pressure in streams 6, see Figure 3.1, changes over the time horizon when the time horizon is fixed.

The other bends occur when separator pressure reach its lower bound, see Figure 6.1 and Figure 6.2. Going back to Section 3.1 the mass flow in the system is given by Equations (3.3) and (3.5). From does two equation the mass flow is given by the pressure drop from the reservoir and well bore-head. So if the pressure drop should decrease the mass flow would decrease. In Equation (3.11) the degeneration of the reservoir pressure is given. Since the reservoir pressure is decreasing and one can not decrease the pressure in the separator it will cause a decrease in pressure drop. Therefore is the second bend caused by the separator pressure reach its lower bound. This is also expected, as the degree of freedom analysis stated that the separator pressure was for controlling the mass flow.

6.2 Results Case 2: Varying Time Horizon

Here are the results from case 2 presented. In this section it is examined how the inclusion of the end time as an additional degree of freedom is effecting the optimal solution.

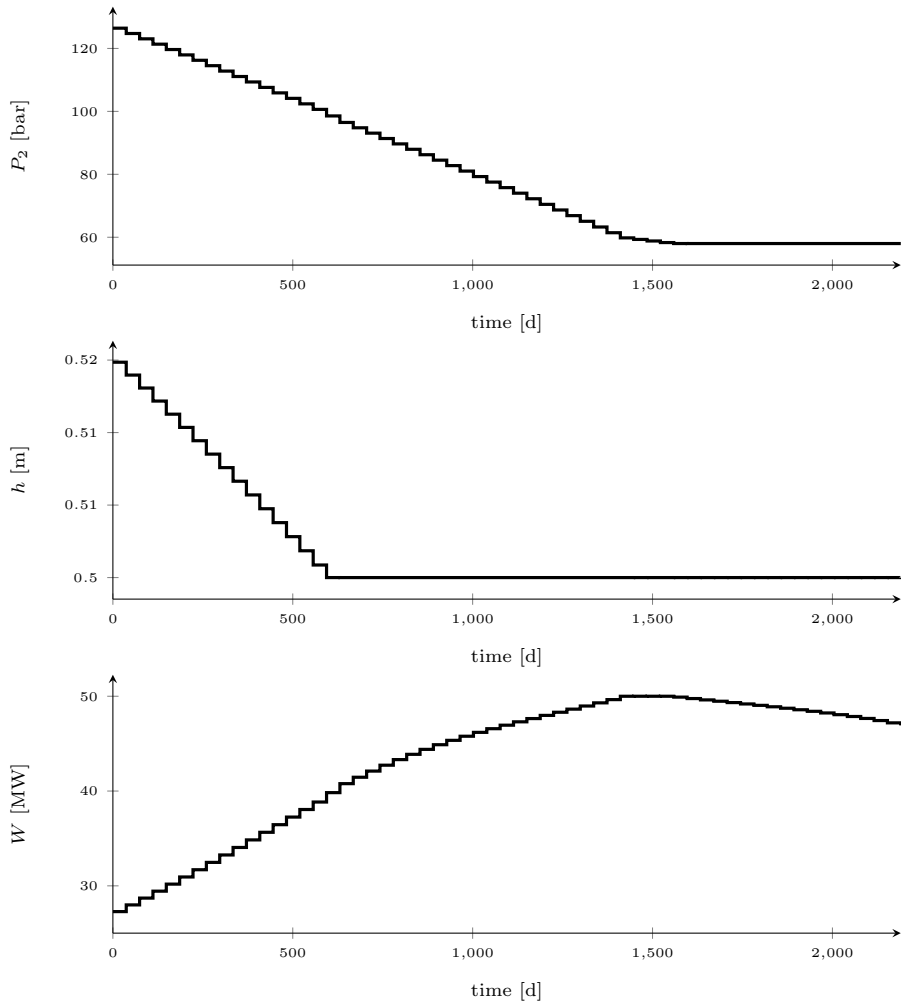

Figure 6.6: The optimal control sequences for the varying time horizon optimization. Where P_2 [bar] is the pressure in the separator, h [m] is the liquid level in the separator and W [MW] is the compressor duty.

In Figure 6.6 the optimal control sequences for the varying time is presented. Comparing the control sequence with the one from case 1, one observers same sequence of arcs in optimal solution, but bends occur at different times. Furthermore, that the time horizon is now 2190 days instead of 1825 days which it was in case 1.

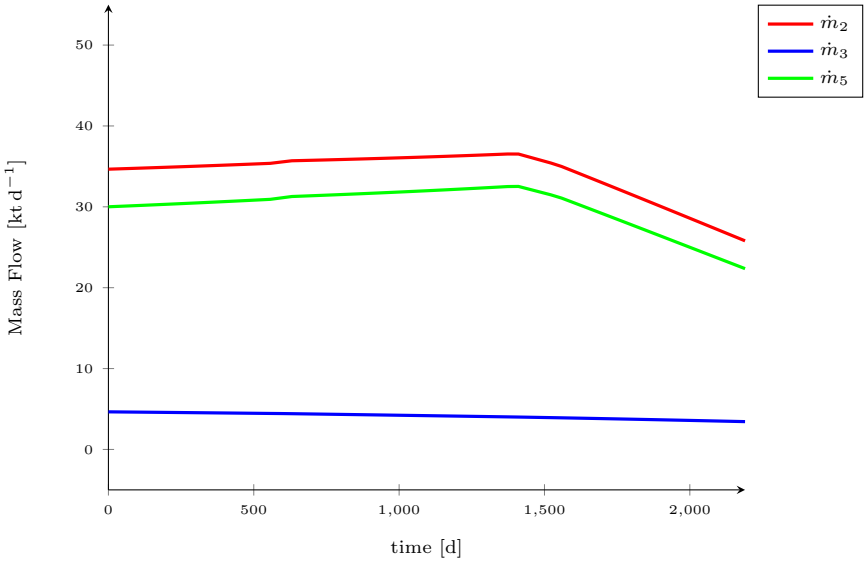

Figure 6.7: The mass flows in and out of the separator, see Figure 3.1, for the optimization with varying time horizon.

The above figure shows the mass flows in and out of the separator for case 2. Comparing the mass flows in case 2 with case 1 that stream 2 and stream 5 are much lower in case 2. But looking at time line in Figure 6.7 that the time horizon is at the upper bound. So the optimizer finds it advantageous to increase the time horizon and decrease the mass flow. In case 1 it was discussed that the gas production was restricted by the lower bound on the compressor efficiency. Also in case 1 it was stated that the oil damaging factor on the compressor was much larger than gas damaging factor. So if one could reduce the oil mass fraction in stream 5 one could produce a great deal more gas. The mass fraction of oil in stream 5 was given by Equation (3.16). In case 1 it was explained that if the liquid level was reduced it would reduce the mass fraction of oil in stream 5. Comparing the liquid level in the separator for the two cases, that in case 1 that the liquid level is a bit higher in the start and is decreased to its lower bound later than in case 2. So it would mean that the mass fraction of oil in stream 5 would be lower in the beginning for case 2. The mass fraction of oil in stream 5 for both case are shown in Figure 6.9, and comparing the two mass fractions that in case 2 it is lower but not only in the beginning. So there is another reason beside the liquid level that the mass fraction is lower in case 2.

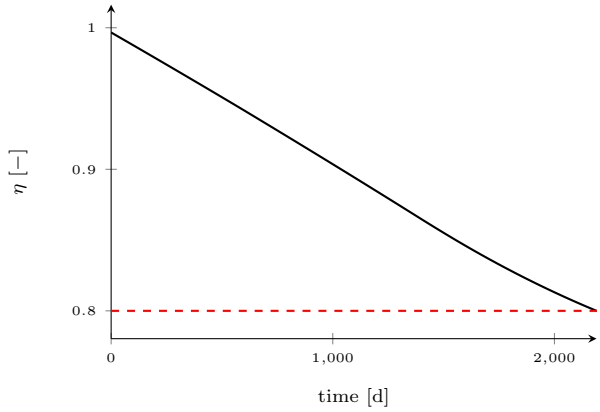

Figure 6.8: The compressor efficiency, η, for the optimizing with varying time.

In Figure 6.8 the compressor efficiency for case 2 is presented. From the graph of the compressor efficiency that it have similarly trajectory as in case 1. This is because the mass flow of stream 5 behaves similarly in both cases, see Figure 6.2 and 6.7. Since the mass flow into the compressor decide the degeneration of the compressor efficiency. The similarly behaviour of the mass flow in the two cases causes the compressor efficiency also to behave similarly for the two cases. The difference is that in case 2 the degeneration is slower as the mass flow is lower.

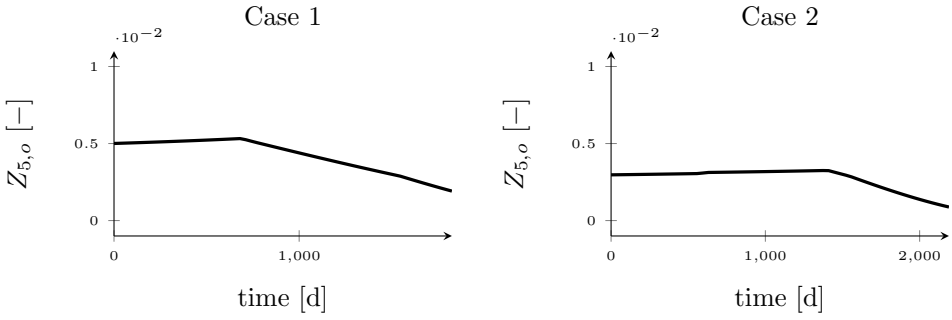

Figure 6.9: The mass fraction of oil in stream 5 for both case 1 and case 2.

The mass fraction of oil was given by Equation (3.16), and it is expressed by the mass fraction in stream 2, volume of the gas phase and the volumetric flow of stream 5. Therefore is it the mass fraction or volumetric flow that causes the mass fraction of oil in stream 5 to be lower in case 2. The volumetric flow is given mass flow divided on the density of the flow. From Figure 6.9 that stream 5 consist of less than one percent oil, so the density is approximately the same in both cases. But since mass flow is much lower in case 2, it means that the volumetric flow lower in case 1 and it is therefore the mass fraction of oil is lower in case 2.

Comparing the mass flow of stream 3 for the two cases, that it is almost the same for both cases. This is because the mass fraction of gas is high in both stream 2 and 5. The gas flow is given by Equation (3.5) and the gas flow is given by quadratic of the pressure difference between the reservoir and well bore-head. While the oil flow which is given by Equation (3.3) the flow is given by the squared of the quadratic pressure difference. This means that gas flow is much more sensitive to the pressure difference between the reservoir and well bore-head. Therefore, in case 2 when the separator pressure is higher it reduces the mass flow of gas more significantly than the mass flow of oil. As stream 3 consists mostly of oil and the mass flow of the stream will not be so much decreased, and therefore will almost be the same in both cases.

6.3 Results Case 3: Net Present Value

For case 3 the net present value (NPV) is included in the objective function, see Equation (5.4). The results are also discussed and compared with the results from the two previous cases.

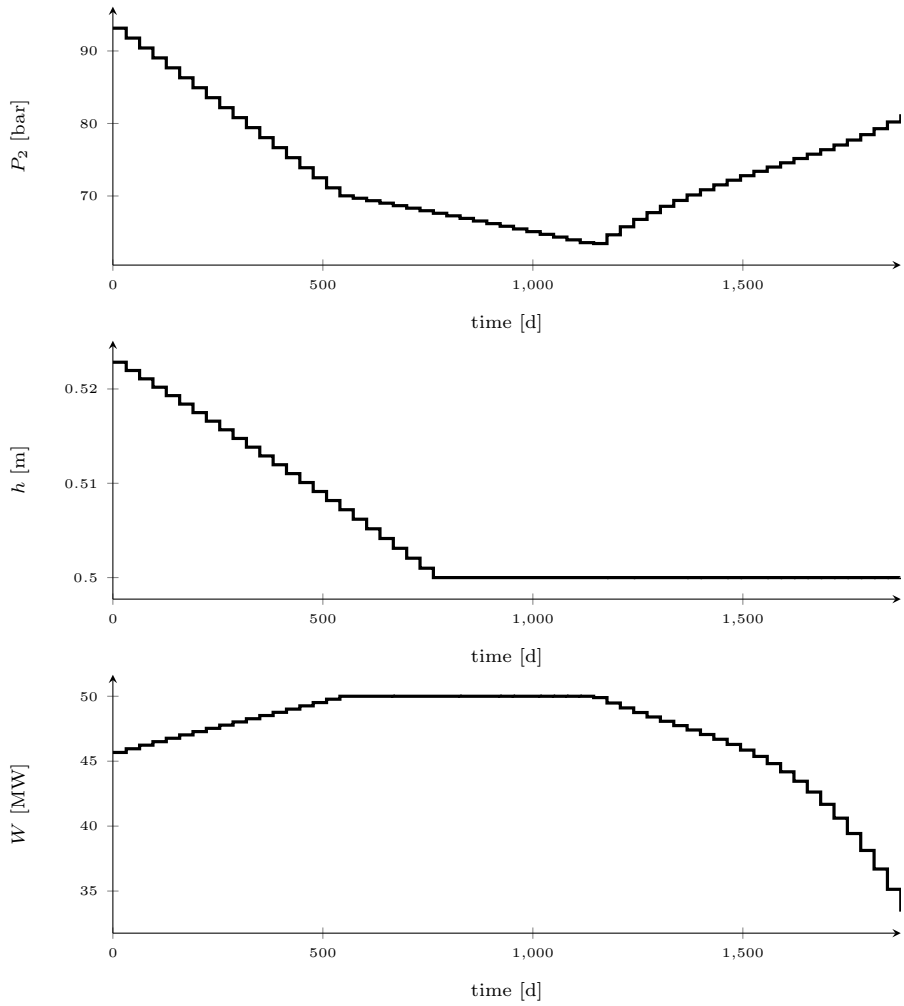

Figure 6.10: The optimal control sequences for case 3, where the net present value is included in the objective function. Where P_2 [bar] is the pressure in the separator, h [m] is the liquid level in the separator and W [MW] is the compressor duty.

From Figure 6.10 that control sequence have similar trajectory as the two previous cases, except in the end where separator pressure starts to increase and the compressor duty decrease significant.

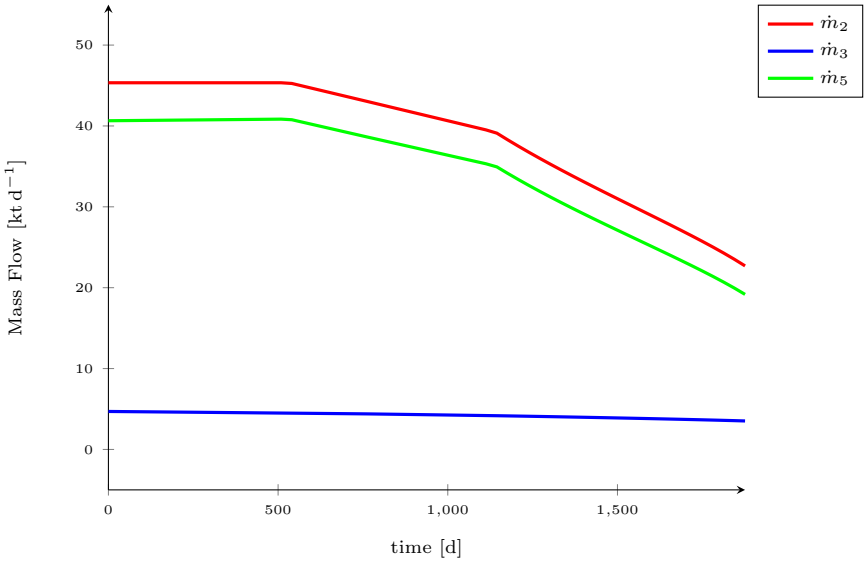

Figure 6.11: The mass flows in and out of the separator, see Figure 3.1, for the optimization of case 3.

In Figure 6.11 the mass in and out of the separator is presented. From the figure one can see that mass flow is at the maximum at the beginning, then starts to decrease. In case 2 the optimizer found it advantageous to decrease the mass flow and increase the time horizon. But in case 3 the optimizer finds it advantageous to maximize production in the start and have lower production in the future. This is expected as in case 3 the value of the gas is higher in the start because of the NPV of the gas. So the trade-off between a increased daily production and increased production time, a increased daily production is favourable in case 3 as it allows for maximum production in the start. This can also been seen by the time horizon in case 3 as it is no longer at the maximum but around 1875 days. Therefore is the separator pressure increasing at the end as one have had an increased production in the start, thereby is the compressor efficiency more reduced so more compensating for this the mass flow needs to be decreased. The compressor efficiency for case 3 is given in Figure 6.12 and here can one see that compressor efficiency is decreasing more in the start then flattens out towards the end such that the lower bound is not violated.

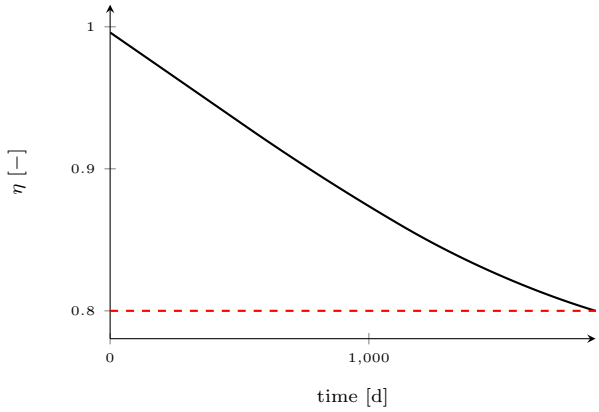

Figure 6.12: The compressor efficiency, η, for the optimizing of case 3.

6.4 Results Case 4: Optimization Under Uncertainty

From the previous cases the deterministic problem was solved with using different objective functions. From the results of those cases, it was found that the overall production of gas was restricted by the lower bound of the compressor efficiency. This bound became active in the end of the time horizon, see Figures 6.3, 6.8 and 6.12. In the beginning of the time horizon the upper bound of the mass fraction of gas in stream is active, see Figure 6.4. The bound is active as it restrict the separation efficiency of oil in the separator. Because of degeneration of the compressor efficiency the lower bound on the pressure in stream 6 becomes active after some time, see Figure 6.5. Lastly, in case 3 the mass flow of stream 2 reaches its upper bound, see Figure 6.11. This is because with the NPV of gas the optimizer finds it advantageous to increase production in the start exchanged for lower production in the future. It is these four constraints that are active when optimizing the subsea separation system. With uncertainty in the reservoir oil flow coefficient these constraint may be violated. Thereafter is it examined if these constraint need a back-off added, which is calculated by use of chance-constraint.

From Section 4.2.4, that for calculating the back-off by use of chance-constraint the probability distribution functions (PDFs) of the variables in the constraint need to be known. Therefore was Monte Carlo simulations executed such that the PDFs of the variables could be approximated. For the PDFs, they were all approximated as Gaussian distributions. For more about the fitting of the PDF see Appendix C.

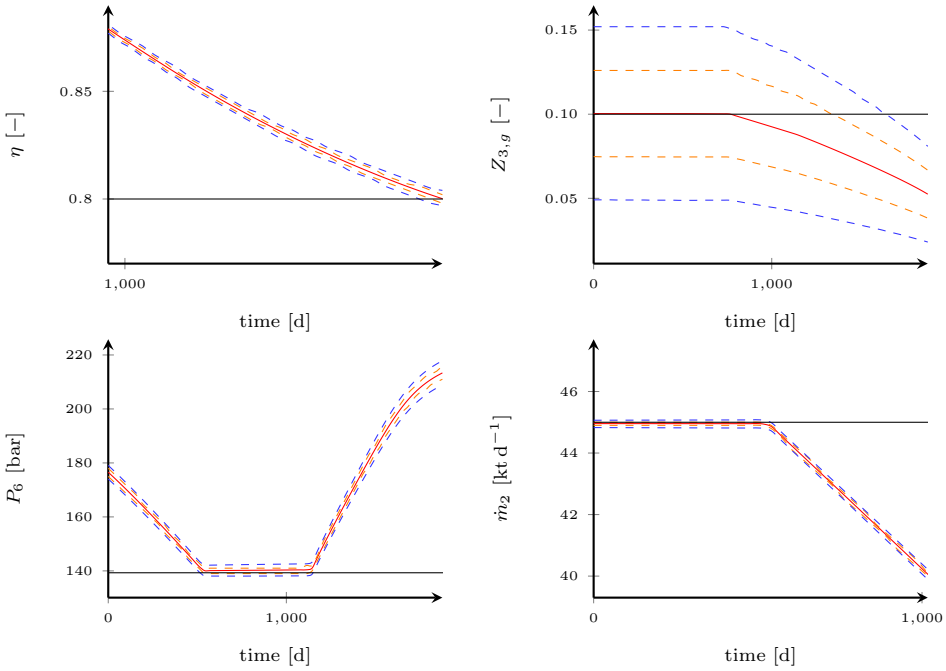

Figure 6.13: The trajectory of the variables that have active constraints given by the red solid line. The variables with active constraint is the compressor efficiency, η, the mass fraction of gas in stream 3, $Z_{3,g}$, the pressure in stream 6, P_6 and the mass flow in stream 2, $\dot{m}_2$. The orange dashed lines indicates one standard deviation from the mean values, while the blue dashed line indicates two standard deviation form the mean value. Then black line is the value of the constraint that becomes active.

In Figure 6.13 the trajectory of the four variable with active constraint are presented with one and two standard deviations. In the upper left corner of Figure 6.13 the compressor efficiency is given. From the plot that the uncertainty increases with the time. The uncertainty in the system is the reservoir oil flow coefficient, which effects the amount of oil out of the reservoir. Therefore will the mass fraction of oil into the separation have an uncertainty. As the amount oil out with the gas phase is given by the mass fraction into the separator, there will be an uncertainty in the amount of oil the compressor processes. The compressor efficiency degeneration is given by the total amount of gas and oil processed, therefore will the uncertainty in the amount of oil processed be accumulated over time. This is the cause for the increase in uncertainty for the compressor efficiency over time. For the mass fraction of gas in stream 3 it is given by the upper right plot in Figure 6.13. From the plot that the uncertainty decreases some after the constraint becomes inactive. As the varaible start to decrease the higher values of variable will decrease more than the lower values. This can be seen in Figure 6.13 by comparing the plot of the two standard deviations, where the plus two standard deviation have a steeper decrease than the minus two standard deviation plot. In the lower left corner of Figure 6.13 the trajectory of the pressure in stream 6 is presented. From the plot one can see that the uncertainty increase

at the end. With the increase of uncertainty in the compressor efficiency, the uncertainty of how effective the compression is increased. Therefore will pressure increase over the compressor have increased uncertainty at the end, which is why the uncertainty increase at the end for the pressure in stream 6. The last plot in Figure 6.13 the mass flow in stream 2 is presented. From the plot that the uncertainty is relative small. Stream 2 consist mostly of gas, while the uncertainty is in the amount of oil in the stream. Therefore will the total mass flow not be as effected by the uncertainty. Further in this work the uncertainty in the mass flow will not considered, as the uncertainty have a negligible effect on the total mass flow of stream 2.

In Figure 6.13 the probability of constraint violation is indicated where the trajectory crosses the black line. For the compressor efficiency that the probability of constraint violation due not occur before the end of the time horizon. This is because compressor efficiency decreases over time and therefore not reaches its lower bound before the end of the time horizon. So adding a chance-constraint at the last lower bound of the compressor efficiency would increase the overall probability of constraint to hold. Therefore will only one chance-constraint be added for the compressor efficiency. For the mass fraction of gas in stream 3 the probability of constraint violation will be 50 % when the constraint is active. Therefore is back-off needed such to reduce the probability of constraint violation. When the constraint is inactive the back-off needed is smaller as the probability of constraint violation is smaller. For the pressure in stream 6 that the mean value is higher than the constraint value. As the mass flow into the separator is not much effected by the uncertainty, see Figure 6.13, the mass flow into the compressor will also not be much effected by the uncertainty. That should make the uncertainty of the pressure in stream 6 relative small, but from Figure 6.13 one can see that this it is larger than the uncertainty of mass flow. This is because the pressure in stream 6 is also effected by the uncertainty in the compressor efficiency. Since the pressure in stream 6 is not much directly effected by the uncertainty, a chance-constraint is not added for the pressure in stream 6. Instead it is presumed that by adding a chance-constraint on the compressor efficiency it will sufficiently decrease the probability of constraint violations for the pressure in stream 6.

With the chance-constraints identified the new OCP can be solved. In Figure 6.14 the control sequence from the OCP with chance-constraint is presented.

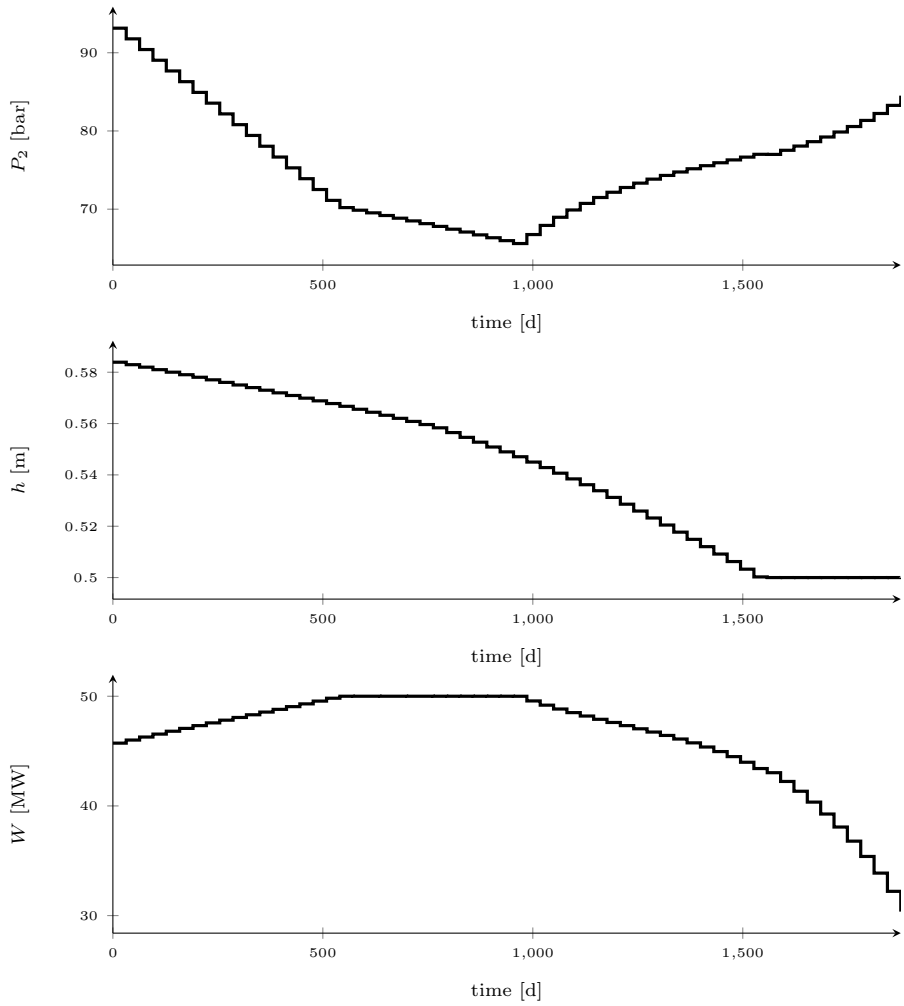

Figure 6.14: The optimal control sequences for case 4, where there are uncertainty in the system. Where P_2 [bar] is the pressure in the separator, h [m] is the liquid level in the separator and W [MW] is the compressor duty.

Comparing the control sequence in Figure 6.14 with the result from case 3, see Figure 6.3, that both the separator pressure and compressor duty have similarly trends. But for the liquid height, the lower bound is reached much later in case 4 than in case 3. The liquid height in the separator was for controlling the mass fraction of gas in stream 3. Since the mass fraction of gas in stream 3 was one of the constraints that a back-off was added such that the probability of the constraint to hold would be higher. Therefore will the upper bound of mass fraction of gas in steam 3 decrease. Thereby must the residence time of the gas in liquid phase be increase, such that one get higher separation of gas. The residence time can be increased by increasing the volume of the liquid phase and therefore is the

liquid level higher in case 4, see Figure 6.14. With a higher liquid level it will take longer to reach its lower bound. Therefore is the lower bound reached later in case 4 than in case 3.

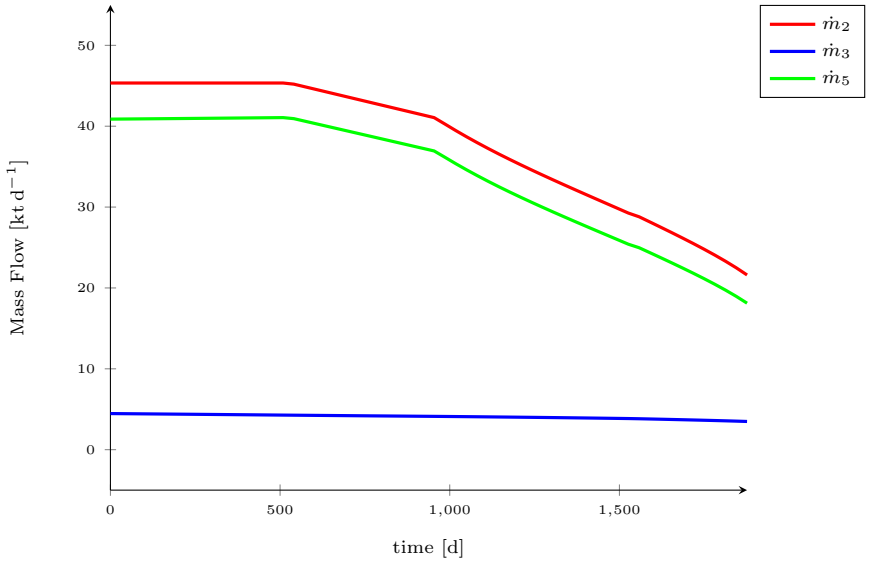

Figure 6.15: The mass flows in and out of the separator, see Figure 3.1, for the optimization of case 34.

In the above figure the mass flows in and out of the separator is presented. Comparing with case 3, see Figure 6.11, the mass flow decreases a little more in case 4. This is because a back-off is added to the lower bound on compressor efficiency, see Figure 6.16, and thereby can the compressor efficiency not be decreased as much as in the previous cases. Therefore must the overall mass flow be decreased. Furthermore in Figure 6.15 that there is small bump after 1500 days. This bump is caused by the liquid level reaches its lower bound, see Figure 6.14. The liquid level can no longer be decreased for keeping the separation efficiency of gas in the separator constant when the mass flow is decreasing, see Figure 6.15. Therefore will the separation efficiency of the gas increased, and more gas will go out with the gas phase. This is the cause of the small bump in the mass flow of stream 5.

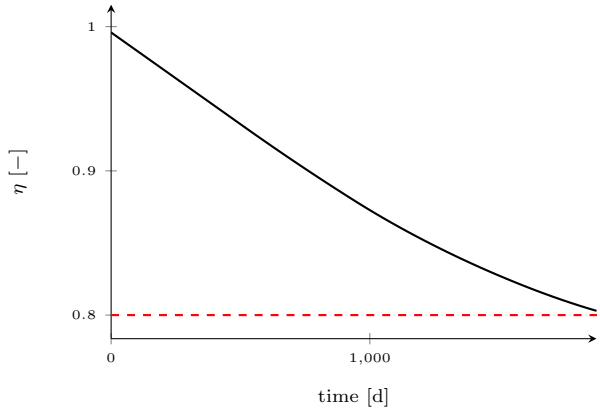

Figure 6.16: The compressor efficiency, η, for the optimizing of case 4.

For the compressor efficiency the trajectory is the same for case 3 and 4, see Figures 6.12 and 6.16. The only difference is that the compressor efficiency do not reach the lower bound in case 4. This is because of the back-off added to the lower bound of the compressor efficiency.

Comparing Figures 6.10 and 6.14, one can see that the optimal control sequence have changed, when one have considered the uncertainty in the system. Therefore will the probability of the active constraint variable also change. For finding the new PDF of the variables Monte Carlo simulation are performed again. The PDF of the variables with active constraint is presented in Figure 6.17.

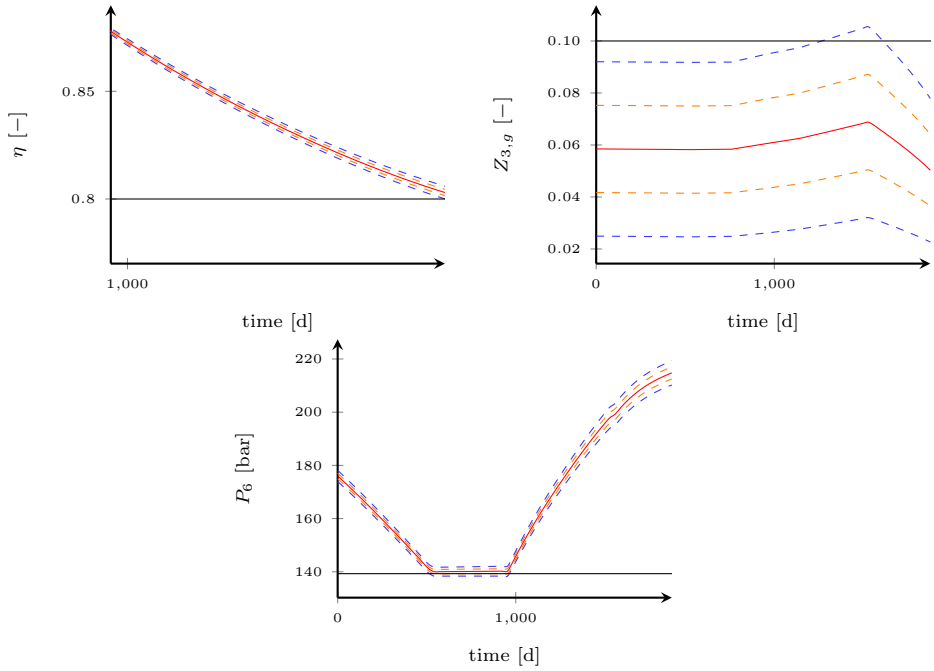

Figure 6.17: The trajectory of the variables that have active constraints given by the red solid line. The variables with active constraint is the compressor efficiency, η, the mass fraction of gas in stream 3, $Z_{3,g}$, the pressure in stream 6, P_6 and the mass flow in stream 2, $\dot{m}_2$. The orange dashed lines indicates one standard deviation from the mean values, while the blue dashed line indicates two standard deviation form the mean value. Then black line is the value of the constraint that becomes active.

Comparing the compressor efficiency curves from Figure 6.13 and 6.17 that the trajectory of the compressor efficiency and pressure in stream 6 have similarly trajectories. For the mass fraction of gas in stream 3 the trajectory increases increases in Figure 6.17 where in Figure 6.17 it decreases. From comparison of the control sequence for case 3 and 4, the liquid level took longer to reach the lower bound in case 4. This means that the upper bound on the mass fraction of gas in stream 3 are longer active. From the the previous discussion in this section, the back-off was reduced when the constraint became inactive as the probability of constraint violation was reduced. Therefore is the back-off to small for the area where the constraint are active in case 4 and not in case 3. Since the back-off is smaller the probability of constraint violation is higher than the probability level, this can be seen in Figure 6.17 where distance between the constraint and second standard deviation is increased. For reducing the probability of constraint violation new back-off needs to be calculated and the OCP need to be solved again, the resulting trajectories and PDF is presented in Figure 6.18.

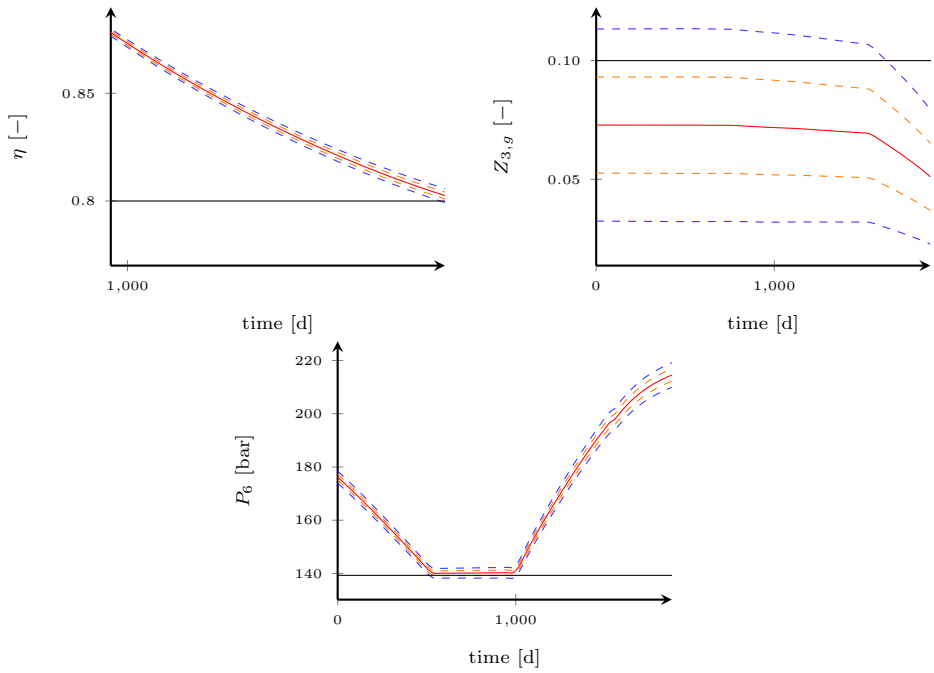

Figure 6.18: The trajectory of the variables that have active constraints given by the red solid line. The variables with active constraint is the compressor efficiency, η, the mass fraction of gas in stream 3, $Z_{3,g}$, the pressure in stream 6, P_6 and the mass flow in stream 2, $\dot{m}_2$. The orange dashed lines indicates one standard deviation from the mean values, while the blue dashed line indicates two standard deviation form the mean value. Then black line is the value of the constraint that becomes active.

From Figure 6.18 that the trajectory of the mass fraction of gas in stream 3, is no longer increasing but have a small decrease instead. This is caused by the probability of constraint violation were high after the first iteration. Thereby was the back-off calculated by the chance-constraint larger for the part of the trajectory were increasing. Therefore is the trajectory decreasing after the second iteration as the back-off calculated is too large.

Comparing Figures 6.17 and 6.18 that the mean value is not the same for the two cases. This is because the back-off calculated for the first OCP with uncertainty is larger than for the second OCP. From comparing Figures 6.10 and 6.14 the optimal solution was changed when back-off was added to the active constraints. Therefore is the PDF of the active variable also changed, therefore is the back-off calculated by the chance-constraint not accurate. This is easily observable from comparing the mass fraction of gas plots in Figures 6.17 and 6.18. In Figure 6.17 the probability of constraint violations is below the second derivation line in the start. While in Figure 6.18 the probability lies between the first and second deviation line. Thereby doing iteration the probability of constraint violation will converge towards the probability level.

For the probability of constraint violation of the pressure in stream 6 that it is the same for all of the cases, see Figures 6.13, 6.17 and 6.18. The reason for no back-off was added to the lower bound of pressure in stream 6 was since the uncertainty was effected the uncertainty of the compressor efficiency. Thereby adding a chance-constraint to the lower bound of the compressor efficiency would decrease the probability of the lower bound of the pressure in stream 6 to be reduced also. This was not the case therefore should chance-constraints also be added for the lower bound of the pressure in stream 6 for reducing the number of constraint violations.

Chapter 7

Conclusion

The purpose of the thesis is to develop a model of a subsea system and to optimize if for operation and remaining life time.First a model of the subsea separation system was developed. Due to no statistical or physical models of the remaining life time of the compressor is available the compressor efficiency was used for indicating the remaining life time of the compressor. Thereafter was a degree of freedom analysis performed. The degree of freedom analysis yielded 3 variables that could be used for control. The variables chosen was the separator pressure, the liquid level in the separator, and the compressor duty. The OCP was formulated, where the profit was given by the amount of gas produced. Four cases was examined, where the three first cases was without uncertainty in the system but with different objective functions. The fourth case, uncertainty in the reservoir flow coefficient was included and how the use of chance-constraint to restrict the probability of constraint violations was examined.

In case 1 the objective function was to maximize the gas production over a fixed time horizon. From the optimization there was three constraint that was active. The lower bound on the compressor efficiency, the upper bound on the mass fraction of gas in stream 3 and the lower bound on the pressure in stream 6. The lower bound on the compressor efficiency is the restriction on the amount of gas produced. The upper bound on the mass fraction of gas in stream 3 restrict the separation efficiency. While the pressure in stream 6 reaches its lower bound because of the degeneration of the compressor efficiency.

For case 2 the end time was introduced as a free variable. With the end time as a free variable the optimizer found it advantageous to decrease the daily production volume but increase the time horizon. This caused the upper bound on the end time to be reached. The decrease of daily production gave an increased separation of oil which reduced the oil damaging term of the compressor degeneration.

For case 3 the NPV of the gas was included in the objective function. The optimization found it advantageous to maximize production of gas in the beginning. This also caused

the time horizon to be reduced to 1875 days.

The last case uncertainty was included in the OCP. The uncertainty was handled with using chance-constraint. For calculating the chance-constraints the PDFs are needed. Monte Carlo simulations was performed for finding the PDFs. From examining the PDFs, the probability of constraint violation was high for the lower bound on the compressor efficiency at the end of the time horizon and for the upper bound on the mass fraction of gas in stream 3. For the pressure in stream 6 and the mass flow the uncertainty in the variables was relative small and therefore was no chance-constraint added for those bound. The OCP was then solved with the back-off calculated from the chance-constraint. The back-off on the upper bound on the mass fraction of gas in stream 3 cause the constraint to be active longer. This caused the probability of constraint violation to be above the probability level. Therefore was new Monte Carlo simulation performed and new back-off calculated. Repeating this process the probability of constraint violations goes towards the the probability level.

The overall conclusion of the thesis is that if there is uncertainty in the system the probability of constraint violation can be controlled by the use of chance-constraint. Thereby can the back-off be reduced such that effectiveness of operation can be increased.

7.1 Future Work

The model of the subsea separation system can be improved upon in some ways:

- Develop a model of the remaining life time of the compressor and implement the model in the OCP.
- Use reservoir statistics from the Ormen Lange field to adjust the reservoir flow coefficients and improve the model of the reservoir pressure degeneration.
- Add extra separation steps or multiple well bore-head in the model.

For the dynamic optimization under uncertainty other methods for handling uncertainty in the optimization should be examined and compared with the chance-constraint method. Monte Carlo simulations are relative slow way of approximating the PDF, therefore should other methods of finding the PDFs be examined.

Bibliography

[1] Andersson, J., 2013. A General-Purpose Software Framework for Dynamic Optimization. Doctor in engineering, Lund University, Sweden.

[2] Bahadori, A., 2014. Natural Gas Processing. Elsevier.
URL http://www.sciencedirect.com/science/article/pii/B9780080999715000040

[3] Bellman, R., 1954. Dynamic Programming and a New Formalism in the Calculus of Variations. Proceedings of the National Academy of Sciences of the United States of America 40 (4), 231–235.
URL http://www.ncbi.nlm.nih.gov/pmc/articles/PMC527981/

[4] Bemporad, A., Morari, M., 1999. Robust model predictive control: A survey. Robustness in identification and control 245, 207—-226.
URL http://link.springer.com/chapter/10.1007/BFb0109870

[5] Ben-tal, A., 2009. On Safe Tractable Approximations of Chance-Constrained Linear Matrix Inequalities. Mathematics of Operations Research 34 (1), 1–25.

[6] Biegler, L. T., 2010. Nonlinear Programming; Concepts, Algorithms, and Applications to Chemical Processes. Society for Industrial and Applied Mathematics, Philadelphia.

[7] Campo, P. J., Morari, M., 1987. Robust Model Predictive Control. In: 1987 American Control Conference. Vol. 2. pp. 1021–1026.
URL www.intechopen.com

[8] Christiansen, H. E., 2012. Rate of Hydrate Inhibitor in Long Subsea Pipelines. Ph.D. thesis, NTNU, NOrway.

[9] Crowe, C., Sommerfeld, M., Tsuji, Y., 1998. Multiphase Flows with Droplets and Particles, 1st Edition. CRC Press, Boca Raton, Florida.

[10] Douc, R., Moulines, E., 2008. Limit theorems for weighted samples with applications to sequential Monte Carlo methods. Annals of Statistics 36 (5), 2344–2376.

[11] Faanes, A., Mordt, H., Eikrem, G. O., Høisæther, K. A., 2007. Process Control of a Subsea Processing Plant. In: 8th International IFAC Symposium on Dynamics and Control of Process Systems. pp. 153–158.
URL http://linkinghub.elsevier.com/retrieve/pii/S147466701531716X

[12] Fantoft, R., 2005. Subsea Gas Compression - Challenges and Solutions. In: Offshore Technology Conference. pp. 1145–1150.

[13] Farina, M., Giulioni, L., Magni, L., Scattolini, R., 2015. Automatica An approach to output-feedback MPC of stochastic linear. Automatica 55, 140–149.
URL http://dx.doi.org/10.1016/j.automatica.2015.02.039

[14] Fetkovich, M. J., 1973. The Isochronal Testing of Oil Wells. In: Annual Fall Meeting of the Society of Petroleum Engineers of AIME. American In8titute of Mining, Metallurgical, and Petroleum Engineer8, Inc. This, Dallas, Texas, p. SPE 4529.

[15] Fishman, G. S., 1996. Monte Carlo. Concepts, Algorithms, and Applications. Springer New York.
URL http://link.springer.com/10.1007/978-1-4757-2553-7

[16] Gaenkoplis, C. J., 2003. Transport Processes and Separation Process Principles, 4th Edition. Pearson Education International.

[17] Gill, P. E., Murray, W., Saunders, M. A., Tomlin, J. A., Wright, M. H., may 2008. George B. Dantzig and systems optimization. Discrete Optimization 5 (2), 151–158.
URL http://www.sciencedirect.com/science/article/pii/S1572528607000321

[18] Golan, M., Whiston, C. H., 1996. Well Performance, 2nd Edition. Tapir akademisk forlag, Trondheim.

[19] Jakobsen, H. A., 2014. Chemical Reactor Modeling Multiphase Reactive Flows. Springer International Publishing.

[20] Langson, W., Chryssochoos, I., Rakoviã C, S. V., Mayne, D. Q., 2004. Robust model predictive control using tubes. Automatica 40, 125–133.
URL www.elsevier.com/locate/automatica

[21] Li, P., Wendt, M., Wozny, G., 2000. Robust model predictive control under chance constraints. Computers & Chemical Engineering 24, 829–834.

[22] Li, P., Wendt, M., Wozny, G., 2002. A probabilistically constrained model predictive controller. Automatica 38 (7), 1171–1176.

[23] Lu, Y., Greene, J., Agrawal, M., 2009. CFD Characterization of Liquid Carryover in Gas / Liquid Separator With Droplet Coalescence due to Vessel Internals. In: SPE Annual Technical Conference and Exhibition. New Orleans, pp. 1332–1346.

[24] Mayne, D. Q., 2014. Model predictive control: Recent developments and future promise. Automatica 50 (12), 2967–2986.
URL http://dx.doi.org/10.1016/j.automatica.2014.10.128

[25] Mcclimans, O. T., Fantoft, R., Technologies, F. M. C., 2006. Status and New Developments in Subsea Processing. Offshore Technology Conference, 1–10.

[26] Mesbah, A., 2016. Stochastic Model Predictive Control : An Overview and Perspectives for Future Research. Tech. rep., Department of Chemical and Biomolecular Engineering, University of California, Berkeley, Berkeley.
URL http://www.cchem.berkeley.edu/mesbah/index{_}files{_}home/Papers/CSM2016{_}In{_}Press.pdf

[27] Morari, M., H. Lee, J., 1999. Model predictive control: past, present and future. Computers & Chemical Engineering 23 (4-5), 667–682.

[28] Moreno-trejo, J., Markeset, T., 2012. Identifying Challenges in the Development of Subsea Petroleum Production Systems. In: IFIP International Federation for Information Processing. pp. 287–295.

[29] Moreno-trejo, J., Markeset, T., 2012. Mapping Factors Influencing the Selection of Subsea Petroleum Production Systems. In: IFIP International Federation for Information Processing 2012. pp. 242–250.

[30] Nocedal, J., Wright, S. J., 2006. Numerical Optimization, 2nd Edition. Springer Science+Business Media.

[31] Oldewurtel, F., Jones, C. N., Morari, M., 2008. A Tractable Approximation of Chance Constrained Stochastic MPC based on Affine Disturbance Feedback. In: 47th IEEE Conference on Deision and Control. Cancun, pp. 4731–4736.

[32] Rakovic, S. V., Kouvaritakis, B., Findeisen, R., Cannon, M., 2012. Homothetic tube model predictive control. Automatica 48 (8), 1631–1638.
URL http://dx.doi.org/10.1016/j.automatica.2012.05.003

[33] Seborg, D. E., Edgar, T. F., Mellichamp, D. A., Doyle III, F. J., 2011. Process Dynamics and Control, 3rd Edition. John Wiley & Sons Ltd.

[34] Sen, S., Higle, J. L., 1999. An Introductory Tutorial on Stochastic Linear Programming Models. Interfaces 29 (2), 33–61.

[35] Skofteland, H., Hilditch, M., Normann, T., Eriksson, K. G., Nyborg, K., Solutions, A., 2009. OTC 20030 Ormen Lange Subsea Compression Pilot Subsea Compression Station. In: Offshore Technology Conference. Houston, Texas, pp. 1–15.

[36] Slettebø, E. S., 2009. Separation of Gas from Liquids in Viscous Systems. Ph.D. thesis, NTNU.

[37] Stewart, M., Arnold, K., 2008. Gas-Liquid And Liquid-Liquid Separators. Elsevier.
URL http://www.sciencedirect.com/science/article/pii/B9780750689793000039

[38] Stuber, M. D., Wechsung, A., Sundaramoorthy, A., Barton, P. I., 2014. Worst-Case Design of Subsea Production Facilities Using Semi-Infinite Programming. AIChE Journal 60 (7), 2513–2524.

[39] Subramaniam, S., 2013. Lagrangian e Eulerian methods for multiphase fl ows. Progrees In Energy and Combustion Science 39 (39).

[40] Valberg, T., 2005. Temperature calculations in production and injection. Master, NTNU.

[41] Vogel, J. V., 1968. Inflow Performance Relationships for Solution-Gas Drive Wells. Society of Petroleum Engineers 243 (1).

[42] Wächter, A., Biegler, L. T., 2006. On the Implementation of Primal-Dual Interior Point Filter Line Search Algorithm for Large-Scale Nonlinear Programming. Mathematical Programming 106 (1), 25–57.
URL http://link.springer.com/10.1007/s10107-004-0559-y$\delimiter"026E30F$nhttp://link.springer.com/article/10.1007/s10107-004-0559-y

[43] Wächter, S., Engineering, C., 1986. Flow in Porous Media I : A Theoretical Derivation of Darcy ' s Law. Transport in Porous Media 1 (1), 3–25.

[44] Zheng, Z., Morari, M., 1993. Robust stability of constrained model predictive control. In: American Control Conference, 1993. pp. 379–383.
URL http://ieeexplore.ieee.org/xpls/abs{_}all.jsp?arnumber=4792879

Appendices

Appendix A

Parameters, Initial Values and Bounds

In this appendix all of the parameters, initial values and variables bounds is given. In Table A.1 the parameters and initial values used in the calculations of the results, which is presented in Sections 6.1-6.2 is given. In Table A.2 the upper and lower bounds used in the optimization is presented.

Table A.1: The parameters used in the calculation.

Variable	Value	Unit	Description
SG_g	0.7	$[-]$	Specific density of gas
SG_0	0.9	$[-]$	Specific density of oil
SG_w	1.0	$[-]$	Specific density of water
ρ_w	1e.3	$\left[\mathrm{kt\,m^{-3}}\right]$	Density of water
g	7.323e10	$\left[\mathrm{m\,d^{-2}}\right]$	Gravitational constant
M	1.604e-5	$\left[\mathrm{kt\,kmole^{-1}}\right]$	Molecular weight of the gas
g_r	0.08314	$\left[\mathrm{bar\,m^3\,K\,kmole}\right]$	Universal gas constant
T_r	374	[K]	Temperature of the reservoir
k_g	1e-5	$\left[\mathrm{kt\,bar^{-3}\,d}\right]$	Reservoir flow coefficient for gas
k_o	1.6e-2	$\left[\mathrm{kt\,bar^{-1}\,d}\right]$	Reservoir flow coefficient for oil
k_w	2.5e-3	$\left[\mathrm{kt\,bar^{-1}\,d}\right]$	Reservoir flow coefficient for water

n	0.5	$[-]$	Dimensionless flow exponential
C	1.5e-4	$\left[\mathrm{bar\,d^{-1}}\right]$	Reservoir pressure degeneration factor
Cv_1	5.5	$\left[\mathrm{kt\,bar^{-0.5}\,d^{-1}}\right]$	Sizing coefficient for valve 1
Cv_1	5.5	$\left[\mathrm{kt\,bar^{-0.5}\,d^{-1}}\right]$	Sizing coefficient for valve 2
y_1	1.0	$[-]$	Valve head position for valve 1
y_2	1.0	$[-]$	Valve head position for valve 2
T_s	274	[K]	Temperature in the separator
L	7.0	[m]	Length of the separator
R	1.5	[m]	Radius of the separator
S_g	2000	$\left[\mathrm{d^{-1}}\right]$	Separation efficiency for gas
S_o	3500	$\left[\mathrm{d^{-1}}\right]$	Separation efficiency for oil
γ	1.31	$[-]$	Heat capacity ratio
A	-3.0e-6	$[\mathrm{kg^{-1}}]$	The gas damaging factor on the compressor
B	-3.0e-5	$[\mathrm{kg^{-1}}]$	The oil damaging factor on the compressor
Pr_0	290	[bar]	Initial value of the reservoir pressure
η_0	1.0	$[-]$	Initial value of η
TF	1875	[d]	Time horizon in days
N	60	$[-]$	Number of time periods

Table A.2: The upper and lower bounds used in the optimization.

Variable	Lower bound	Upper Bound	Unit
$\dot{m}_g$	0.0	45.34	$\left[\mathrm{kt\,d^{-1}}\right]$
$\dot{m}_o$	0.0	45.34	$\left[\mathrm{kt\,d^{-1}}\right]$
$\dot{m}_w$	0.0	45.34	$\left[\mathrm{kt\,d^{-1}}\right]$
$\dot{m}_1$	0.0	45.34	$\left[\mathrm{kt\,d^{-1}}\right]$
$\dot{m}_2$	0.0	45.34	$\left[\mathrm{kt\,d^{-1}}\right]$
$\dot{m}_3$	0.0	45.34	$\left[\mathrm{kt\,d^{-1}}\right]$

$\dot{m}_4$	0.0	45.34	$\left[\mathrm{kt\,d^{-1}}\right]$
$\dot{m}_5$	0.0	45.34	$\left[\mathrm{kt\,d^{-1}}\right]$
$\dot{m}_6$	0.0	45.34	$\left[\mathrm{kt\,d^{-1}}\right]$
$Z_{1,g}$	0.0	1.0	$[-]$
$Z_{1,o}$	0.0	1.0	$[-]$
$Z_{1,w}$	0.0	1.0	$[-]$
$Z_{2,g}$	0.0	1.0	$[-]$
$Z_{2,o}$	0.0	1.0	$[-]$
$Z_{2,w}$	0.0	1.0	$[-]$
$Z_{3,g}$	0.0	0.1	$[-]$
$Z_{3,o}$	0.0	1.0	$[-]$
$Z_{3,w}$	0.0	1.0	$[-]$
$Z_{4,g}$	0.0	1.0	$[-]$
$Z_{4,o}$	0.0	1.0	$[-]$
$Z_{4,w}$	0.0	1.0	$[-]$
$Z_{5,g}$	0.0	1.0	$[-]$
$Z_{5,o}$	0.0	0.01	$[-]$
$Z_{6,g}$	0.0	1.0	$[-]$
$Z_{6,o}$	0.0	1.0	$[-]$
P_{wf}	0.0	290	[bar]
P_1	0.0	290	[bar]
P_2	58.0	290	[bar]
P_3	0.0	290	[bar]
P_4	0.0	290	[bar]
P_5	0.0	290	[bar]
P_6	140	290	[bar]
V_l	0.0	49.5	$\left[\mathrm{m^3}\right]$
ρ_3	0.0	1.0e-3	$\left[\mathrm{kt\,m^{-3}}\right]$
ρ_5	0.0	1.0e-3	$\left[\mathrm{kt\,m^{-3}}\right]$

η	0.8	1.0	$[-]$
h	0.5	2.5	$[\mathrm{m}]$
W	0.0	50	$[\mathrm{MW}]$
T_f	1460	2190	$[\mathrm{d}]$

Appendix B

Parameter Adjustment

The parameters in Table B.1 was not found in the literature but are fitted such that system operates similarly to the Ormen Lange field. How this parameters was fitted is described in this appendix.

Table B.1: The parameters that are not found in literature but fitted from operation data from the Ormen Lange field.

Variable	Unit	Description
k_g	$\left[\mathrm{kt\,bar^{-3}\,d}\right]$	Reservoir flow coefficient for gas
k_o	$\left[\mathrm{kt\,bar^{-1}\,d}\right]$	Reservoir flow coefficient for oil
k_w	$\left[\mathrm{kt\,bar^{-1}\,d}\right]$	Reservoir flow coefficient for water
Cv_1	$\left[\mathrm{kt\,bar^{-0.5}\,d^{-1}}\right]$	Sizing coefficient for valve 1
Cv_1	$\left[\mathrm{kt\,bar^{-0.5}\,d^{-1}}\right]$	Sizing coefficient for valve 2
S_g	$\left[\mathrm{d^{-1}}\right]$	Separation efficiency for gas
S_o	$\left[\mathrm{d^{-1}}\right]$	Separation efficiency for oil
A	$[\mathrm{d^{-1}}]$	The gas damaging factor on the compressor
B	$[\mathrm{d^{-1}}]$	The oil damaging factor on the compressor
C	$\left[\mathrm{bar\,d^{-1}}\right]$	Reservoir pressure degeneration factor

For calculating the mass flow of gas, oil and water from the reservoir the reservoir flow coefficients needed to be fitted. From literature the composition of the Ormen Lange reservoir is given in [8]. Assuming that methane and components with lower molar weight are

gas while those components with higher molar weight are oil, the mass fraction of gas, oil and water was found. With the mass fraction the ratio between the gas, oil and water flows is given. Furthermore the maximum production of gas is given in [35]. Thereby using the mass fractions and max production the reservoir flow coefficients can be found from Equations (3.3) and (3.5) if the pressure drop from the reservoir to the well bore-head is known. Assuming that the reservoir was 290 bar the pressure at the well bore-head was 160 and bars the three flow coefficient was fitted such that the total mass flow was equal to the maximum gas production.

For the sizing coefficient of the valves they gives the pressure drop over the valves. For the pressure drop over the first valve it would represent the pressure drop that would have been if one include, choke valve, christmas tree, pipe lines etcetera into the model. From [35] it is given that the pressure into the separator is 80 bar, therefore assuming with a pressure of 80 bars in the separator that one have maximum production. The using Equation (3.12) and assuming that the valve is fully open the valve sizing coefficient for the first valve was calculated. For the second valve the valve coefficient was found such that it equalled the increase of pressure because of the liquid in the separator, when the height of the liquid is equal to 1 meter.

The amount of gas carryunder and oil carryover is decided by the separation coefficients. For finding those parameters the model equations of the separator was solved. Where one assumed that the mass flow of stream 3 was equal to the mass flow of oil and water into the separator under maximum production properties.

For A and B those was found from the assumption that under maximum production of gas the compressor efficiency would decreas with 25 percent if only gas was compressed. Then assuming that the damaging factor of oil was ten times larger then for gas. For the C is was fitted such that over a 5 years period the pressure would decrease with around 20 percent.

Appendix C

Probability Distribution Fitting

In this chapter the probability fitting of the outcome for compressor efficiency, mass fraction of gas in stream 3, pressure in stream 6 and the mass flow in stream 2 from the Monte Carlo simulation is presented in Figures C.1-C.4. For the Monte Carlo simulation 1000 simulations was preformed. In the figures the green bars is the histogram of the outcome from the simulations, while the red line is the approximated PDF. From the figures that the approximation of a normal distribution is a good fit for all of the variables. For the pressure in stream 6 and mass flow in stream 2 the variables are made dimensionless in the calculation and is therefore between one and zero. The variables was made dimensionless by dividing on the upper bounds.

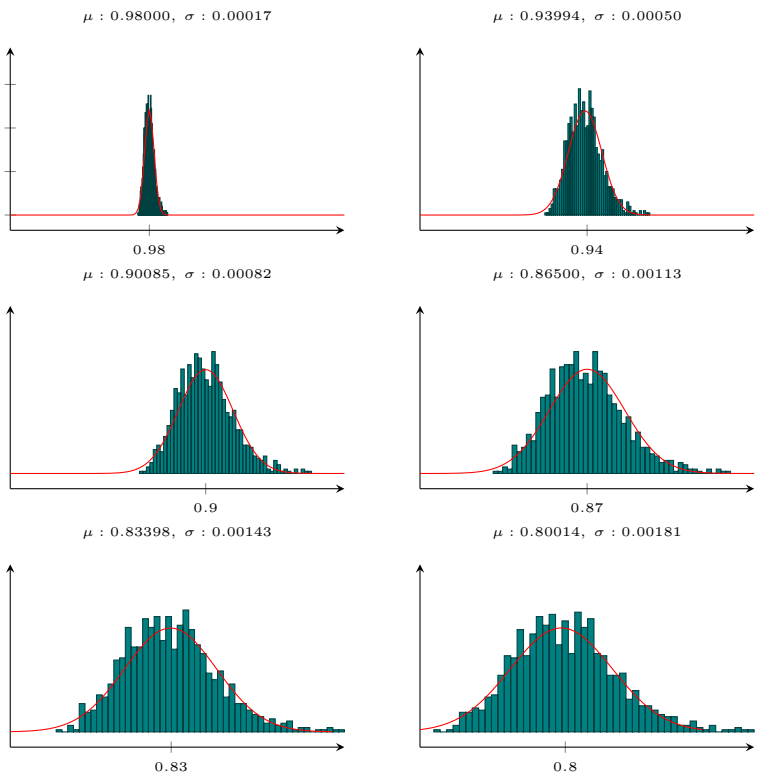

Figure C.1: Histogram of the outcome of the compressor efficiency, η, from the Monte Carlo simulation, with the red line indicating the normal distribution fitting of the outcomes. The histogram is made for time periods 155 days, 465 days, 775 days, 1085 days, 1395 days and 1875 days, from left to right and top to bottom.

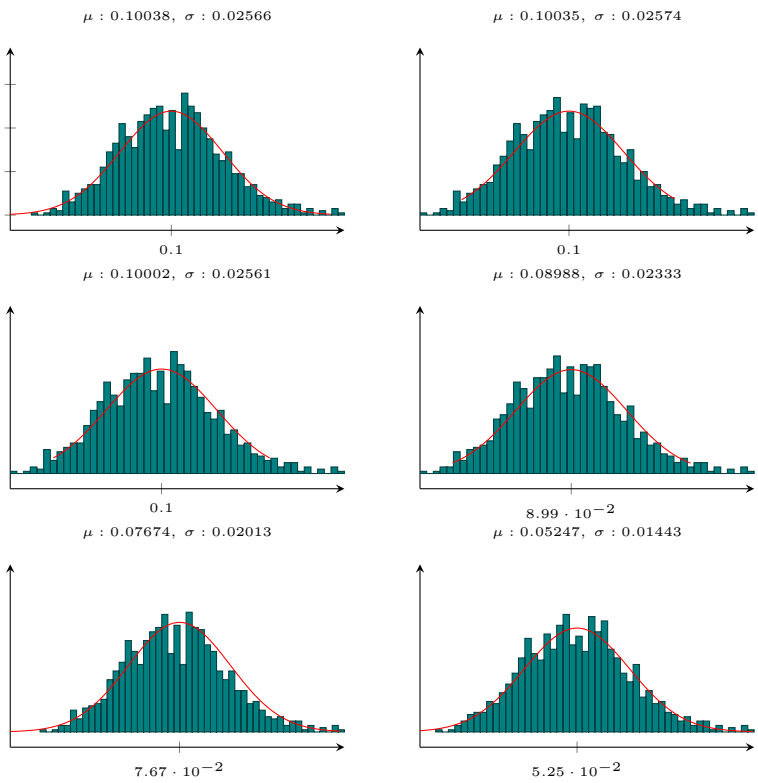

Figure C.2: Histogram of the outcome of the mass fraction of gas in stream 3, $Z_{3,g}$, from the Monte Carlo simulation, with the red line indicating the normal distribution fitting of the outcomes. The histogram is made for time periods 155 days, 465 days, 775 days, 1085 days, 1395 days and 1875 days, from left to right and top to bottom.

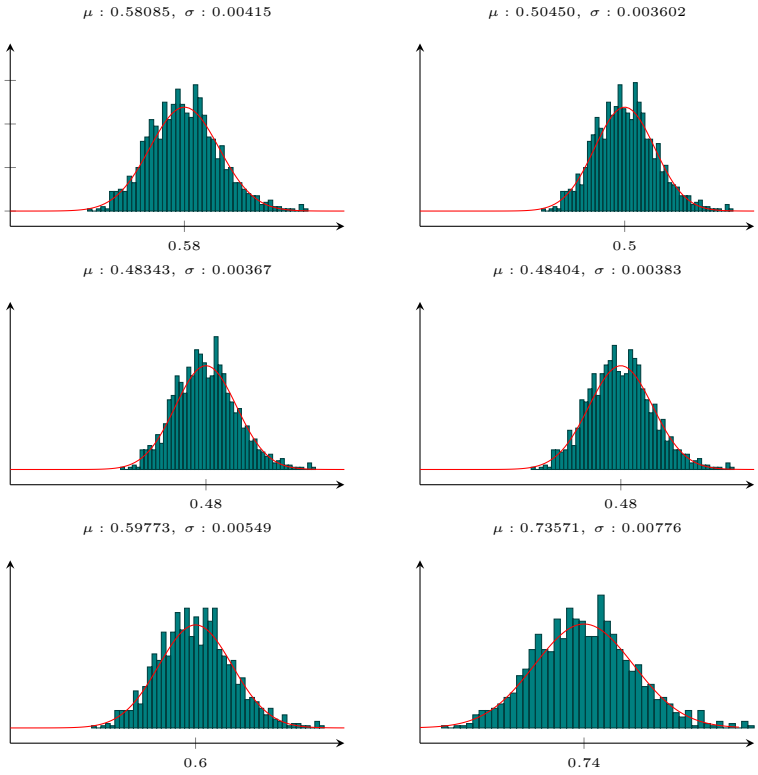

Figure C.3: Histogram of the outcome of the pressure in stream 6, P_6, from the Monte Carlo simulation, with the red line indicating the normal distribution fitting of the outcomes. The histogram is made for time periods 155 days, 465 days, 775 days, 1085 days, 1395 days and 1875 days, from left to right and top to bottom.

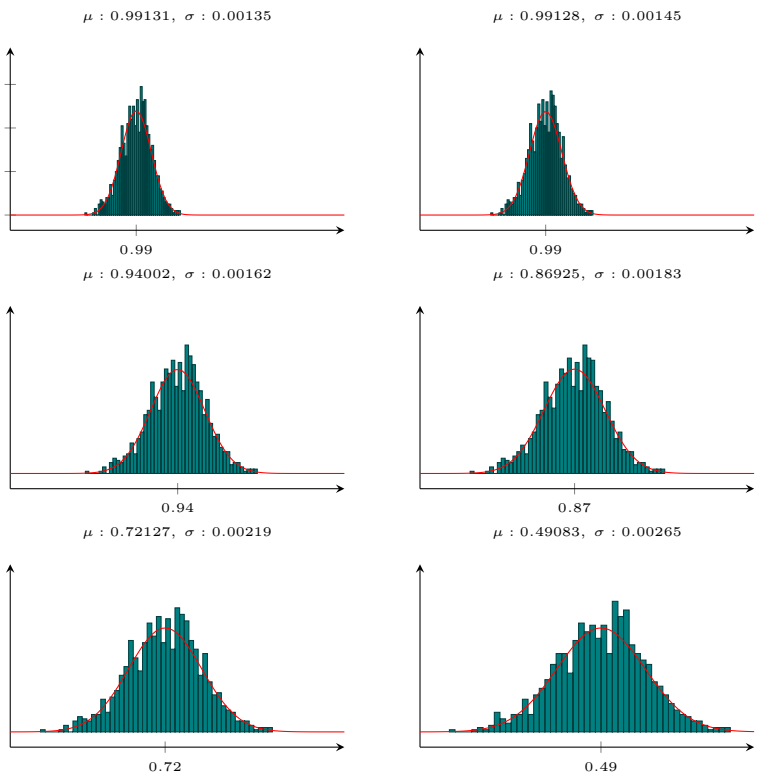

Figure C.4: Histogram of the outcome of the mass flow in stream, $\dot{m}_2$, from the Monte Carlo simulation, with the red line indicating the normal distribution fitting of the outcomes. The histogram is made for time periods 155 days, 465 days, 775 days, 1085 days, 1395 days and 1875 days, from left to right and top to bottom.

Appendix D

Python Code

Here is all of the python codes used for in the calculations of the results.

D.1 Parameter

```
from math import pi

def Parameters():
        class para():
                "Parameters and initial conditions"
                pass
        p = para()
        # Initial conditions
        p.Pr_0 = 1.0 # Pressure in the reservior [-]
        p.eta0 = 1.0 # Starting value for compressor efficiency
        # Valve parameters
        p.Cv1 = 5.5 # Valve 1 sizing coeficient [kt/bar^(1/2) d]
        p.Cv2 = 3.5 #  Valve 2 sizing coeficient [kt/bar^(1/2) d]
        p.u1 = 1.0
        p.u2 = 1.0
        # Separator
        p.L = 7.0 # Length of separator [m]
        p.R = 1.5 # Radius of Separator [m]
        p.V = pi*p.L*p.R**2 # Volume of separator [m^3]
        p.Sep_o = 3500.0 # Separator performance constant for oil
            separation [1/d]
        p.Sep_g = 2000.0 # Separator performance constant for gas
            separation [1/d]
        # Compressor
        p.gamma = 1.31 # the ratio of heat capacities (methane)
        p.A = -3.0e-6 # [1/t]
        p.B = -3.0e-5 # [1/t]
        p.P6 = 0.4828 # Pressure after the compression [bar]
        # Reservoir
        p.C = -1.5e-4 # Pressure change with respect to time constant
        p.ko = 0.0160 # [kt/bar d]
```

```
    p.kw = 0.0025 # [kt/bar d]
    p.kg = 1.0e-5 # [kt/bar^3 d]
    p.n = 0.5 # dimesionless constant for Fetkovich equation
    p.Delta_h = -2000 # Height from reservoir to the seabed [m]
    # Data
    p.SG_g = 0.7 # Specific gravity gass [-]
    p.SG_o = 0.9 # Specific gravity oil [-]
    p.SG_w = 1.0 # Specific gravity water [-]
    p.rho_w = 1.0e-3 # Density water [kt/m^3]
    p.g = 7.323e10 # Gravitational constant [m/d^2]
    p.Rg = 0.08314 # Gas constant [bar m^3 / K kmole]
    p.Tr = 374.0 # Temperature in the reservoir [K]
    p.Ts = 274.0 # Temperature in the separator [K]
    p.M = 1.604e-5 # Molecular weight methane [kt/kmol]
    p.N = 60 # Number of intergration points
    p.TF = 1825.0 # End time [d]
    p.Pa_Bar = 1.33959e-9 # Convert from kt/m d^2 to bar
    p.d = 5 # Degree of interpolating polynomial
    p.m_max = 45.34 # Maximum production [kt/d]
    p.P_max = 290.0 # Maximum pressure [bar]
    p.V_max = p.V # Maximum volume of liquid in the separator [m^3]
    p.rho_max = 1.0e-3 # Maximum density [kt/m^3]
    p.W_max = 50.0 # Maximum compressor duty [Mw]
    p.P2 = 0.35
    p.h = 1.0
    p.W = 0.45
    p.On = 1 # 1 end time is a variable, 0 end time is fixed
    p.PV = 1 # Present value on/off.
    p.ns = 1000 # Number of simulations
    p.tx = 2 + p.d*2 # Starting position of the algebraic variables
    p.tz = p.tx + 34*p.d # Starting position of the Control variables
    return p
```

D.2 Model Equations

```
from math import pi
from casadi import *
import numpy as np

def Model(p):
    # End time variables
    t_end = SX.sym("t_end")
    # Algebraic variables
    # Mass variables
    m_g = SX.sym("m_g")
    m_o = SX.sym("m_o")
    m_w = SX.sym("m_w")
    m1 = SX.sym("m1")
    m2 = SX.sym("m2")
    m3 = SX.sym("m3")
    m4 = SX.sym("m4")
    m5 = SX.sym("m5")
    m6 = SX.sym("m6")
    # Mass fraction variables
    Z1_g = SX.sym("Z1_g")
    Z1_o = SX.sym("Z1_o")
```

```
Z1_w = SX.sym("Z1_w")
Z2_g = SX.sym("Z2_g")
Z2_o = SX.sym("Z2_o")
Z2_w = SX.sym("Z2_w")
Z3_g = SX.sym("Z3_g")
Z3_o = SX.sym("Z3_o")
Z3_w = SX.sym("Z3_w")
Z4_g = SX.sym("Z4_g")
Z4_o = SX.sym("Z4_o")
Z4_w = SX.sym("Z4_w")
Z5_g = SX.sym("Z5_g")
Z5_o = SX.sym("Z5_o")
Z6_g = SX.sym("Z6_g")
Z6_o = SX.sym("Z6_o")
# Pressure
Pwf = SX.sym("Pwf")
P1 = SX.sym("P1")
P3 = SX.sym("P3")
P4 = SX.sym("P4")
P5 = SX.sym("P5")
# Other variables
V_l = SX.sym("V_l") # Liquid volume in the separator [m^3]
rho_3 = SX.sym("rho_3") # Density of stream 3 [kt/m^3]
rho_5 = SX.sym("rho_5") # Density of stream 5 [kt/m^3]
P6 = SX.sym("P6") # Pressure stream 6 [bar]

# Collect all the algebraic variables into a vector
z = vertcat(m_g,m_o,m_w,m1,m2,m3,m4,m5,m6,
                        Z1_g,Z1_o,Z1_w,Z2_g,Z2_o,Z2_w,Z3_g,Z3_o,
                            Z3_w,
                        Z4_g,Z4_o,Z4_w,Z5_g,Z5_o,Z6_g,Z6_o,
                        Pwf,P1,P3,P4,P5,
                        V_l,rho_3,rho_5,P6)
# Differential variables
eta = SX.sym("eta")
Pr = SX.sym("Pr")
x = vertcat(Pr,eta)
# Control Variables
P2 = SX.sym("P2")
h = SX.sym("h")
Ws = SX.sym("Ws") # Work done by compressor [MW]
u = vertcat(P2,h,Ws)

# algebraic equations
# Resevoir
eq27 = P1 - Pwf - (p.Pa_Bar)*(m1*p.g*p.Delta_h*Pwf)/ \
                (       (m_g*p.Rg*p.Tr/p.M) + p.P_max*Pwf*(m_o/(p.
                    rho_w*p.SG_o) \
                + m_w/p.rho_w)) # Pressure drop from reservoir to
                    seabed [bar]
eq28 = m_o - (p.ko/p.m_max)*((p.P_max*Pr)**2 - (p.P_max*Pwf)**2)**
    p.n # Mass flow of oil in stream 1 [kt/tau]
eq29 = m_w - (p.kw/p.m_max)*((p.P_max*Pr)**2 - (p.P_max*Pwf)**2)**
    p.n # Mass flow of water in stream 1 [kt/tau]
eq30 = m_g - m_o*(p.kg/p.ko)*(p.P_max*Pr - p.P_max*Pwf)**2 # Mass
    flow of gas in stream 1 [kt/tau]
eq31 = m1 - m_g - m_o - m_w # Total mass flow in stream 1 [kt/tau]
```

```
eq32 = Z1_g - m_g/m1 # Mass fraction of gas in stream 1
eq33 = Z1_o - m_o/m1 # Mass fraction of oil in stream 1
eq34 = Z1_w - m_w/m1 # Mass fraction of water in stream 1

# Valve1
eq1 = m1 - m2 # constant mass flow over valve1
eq2 = m2 - p.u1*p.Cv1/p.m_max*sqrt((p.P_max*(P1-P2))/(Z1_g*p.SG_g
    \
                + Z1_o*p.SG_o + Z1_w*p.SG_w)) # Mass flow out of
                    the valve [-]
eq3 = Z1_g - Z2_g # Mass fraction constant over valve
eq4 = Z1_o - Z2_o # Mass fraction constant over valve
eq5 = Z1_w - Z2_w # Mass fraction constant over valve

# Separator
eq6 = m2 - m3 - m5 # total mass balance over the separator
eq7 = Z2_g*m2 - Z3_g*m3 - Z5_g*m5 # mass balance gass
eq8 = Z2_o*m2 - Z3_o*m3 - Z5_o*m5 # mass balance oil
eq9 = Z5_o - Z2_o*exp(-p.Sep_o*((p.V-V_l*p.V_max)/((p.m_max*m5)/(p
    .rho_max*rho_5)))) # Mass fraction of oil as function of
    separator efficiecny and resident time.
eq10 = Z3_g - Z2_g*exp(-p.Sep_g*((V_l*p.V_max)/((p.m_max*m3)/(p.
    rho_max*rho_3)))) # Mass fraction of gas as function of
    separator efficiecny and resident time.
eq11 = Z5_g + Z5_o  - 1 # mass fractions equal to 1 for stream 5
eq12 = Z3_g + Z3_o + Z3_w - 1 # mass fractions equal to 1 for
    stream 3
eq13 = P2 - P5 # No pressure drop over the separator
eq14 = P3 - P2 - (p.rho_max/p.P_max)*rho_3*p.g*h*(p.Pa_Bar) #
    Pressure in outlet stream 3 [-]
eq15 = rho_3 - (p.rho_w/p.rho_max)*( Z3_g*p.SG_g + Z3_o*p.SG_o +
    Z3_w*p.SG_w) # Density stream 3 [-]
eq16 = rho_5 - (p.rho_w/p.rho_max)*(Z5_g*p.SG_g + Z5_o*p.SG_o ) #
    Density stream 3 [-]
eq17 = V_l - p.L*((h - p.R)*sqrt(2*p.R*h-h**2) + p.R**2*acos(1.0-h
    /p.R))*(1.0/p.V_max) # Volume of liquid in the separator [-]

# Valve2
eq18 = m3 - m4 # Mass balance over valve [kt/tau]
eq19 = m4 - (p.u2*p.Cv2/p.m_max)*sqrt((p.P_max*(P3-P4))/(Z3_g*p.
    SG_g \
                + Z3_o*p.SG_o + Z3_w*p.SG_w)) # Mass flow out of
                    the valve
eq20 = Z3_g - Z4_g # Mass fraction constant over valve
eq21 = Z3_o - Z4_o # Mass fraction constant over valve
eq22 = Z3_w - Z4_w # Mass fraction constant over valve


# Compressor
eq23 = m5 - m6 # mass flow constant over compressor
eq24 = Z5_g - Z6_g # Mass fraction constant over compressor
eq25 = Z5_o - Z6_o # Mass fraction constant over compressor
eq26 = Ws - (p.gamma/(p.gamma - 1))*((p.Rg*p.Ts/p.M)*((P6/P5)**((p
    .gamma-1)/p.gamma) \
                -1))*((m5*p.m_max)/(p.W_max*p.eta0))*1.1574e-6 #
                    Compressor duty [MW]
```

```
        # Collect all of the algebraic equations into a vector
        f = vertcat(eq30,eq28,eq29,eq31,eq1,eq6,eq18,eq7,eq23,
                                        eq32,eq33,eq34,eq3,eq4,eq5,eq10,
                                            eq8,eq12,
                                        eq20,eq21,eq22,eq11,eq9,eq24,eq25,
                                        eq27,eq2,eq14,eq19,eq13,
                                        eq17,eq15,eq16,eq26)
        if p.On == 1:
                # Differential equations
                dPrdt = p.TF*t_end*p.C # Pressure decrease
                detadt = p.TF*t_end*(p.A*m5*p.m_max*Z5_g + p.B*m5*p.m_max*
                    Z5_o) # Change of compressor efficiency
                dx = vertcat(dPrdt,detadt)

                # Objective function
                obj =   - m6*Z6_g  # objective function

        else:
                # Differential equations
                dPrdt = p.TF*p.C # Pressure decrease
                detadt = p.TF*(p.A*m5*p.m_max*Z5_g + p.B*m5*p.m_max*Z5_o)
                    # Change of compressor efficiency
                dx = vertcat(dPrdt,detadt)

                # Objective function
                obj =   - m6*Z6_g # objective function
        return f,dx,obj,x,z,u,t_end
```

D.3 Initial Guess

```
from math import pi
from casadi import *
import numpy as np
from Layout import Layout
from Model import Model
from collections import OrderedDict
from helpers import casadi_vec, casadi_struct, casadi_vec2struct,
    casadi_struct2vec


def Initial(p,z,V_block):
        [f,dx,obj,x,z,u,t_end] = Model(p);
        [Int,dae,dae,dae_x,dae_z,dae_u,tau_root,dae_t_end] = Layout(p,f,dx
            ,obj,x,z,u,t_end);
        init = []
        u = [p.P2,p.h,p.W]
        U_init = u
        # ts = ([0] + collocation_points(p.d, 'radau') )
        # t = [x/p.N for x in ts]
        # print t
        # t = [0] + collocation_points(p.d, 'radau')
        for i in range(p.N):

                if i == 0:
                        x = [p.Pr_0,p.eta0]
```

```
        X_init = x

# algebraic equations
# Resevoir
eq27 = z[26] - z[25] - (p.Pa_Bar)*(z[3]*p.g*p.Delta_h*z
    [25])/ \
                        ((z[0]*p.Rg*p.Tr/p.M) + p.P_max*z
                            [25]*(z[1]/(p.rho_w*p.SG_o) \
                        + z[2]/p.rho_w)) # Pressure drop
                            from reservoir to seabed [bar]
eq28 = z[1] - (p.ko/p.m_max)*((p.P_max*x[0])**2 - (p.P_max
    *z[25])**2)**p.n # Mass flow of oil in stream 1 [-]
eq29 = z[2] - (p.kw/p.m_max)*((p.P_max*x[0])**2 - (p.P_max
    *z[25])**2)**p.n # Mass flow of water in stream 1 [-]
eq30 = z[0] - z[1]*(p.kg/p.ko)*(p.P_max*x[0] - p.P_max*z
    [25])**2 # Mass flow of gas in stream 1 [-]
eq31 = z[3] - z[0] - z[1] - z[2] # Total mass flow in
    stream 1 [-]
eq32 = z[9] - z[0]/z[3] # Mass fraction of gas in stream 1
eq33 = z[10] - z[1]/z[3] # Mass fraction of oil in stream
    1
eq34 = z[11] - z[2]/z[3] # Mass fraction of water in
    stream 1

# Valve1
eq1 = z[3] - z[4] # constant mass flow over valve1
eq2 = z[4] - (p.u1*p.Cv1/p.m_max)*sqrt((p.P_max*(z[26]-u
    [0]))/(z[9]*p.SG_g \
                        + z[10]*p.SG_o + z[11]*p.SG_w)) #
                            Mass flow out of the valve [kt
                            /tau]
eq3 = z[9] - z[12] # Mass fraction constant over valve
eq4 = z[10] - z[13] # Mass fraction constant over valve
eq5 = z[11] - z[14] # Mass fraction constant over valve


# Separator
eq6 = z[4] - z[5] - z[7] # total mass balance over the
    separator
eq7 = z[12]*z[4] - z[15]*z[5] - z[21]*z[7]  # mass balance
     gass
eq8 = z[13]*z[4] - z[16]*z[5] - z[22]*z[7] # mass balance
    oil
eq9 = z[22] - z[13]*exp(-p.Sep_o*((p.V-z[30]*p.V_max)/ \
        ((p.m_max*z[7])/(p.rho_max*z[32])))) # Mass
            fraction of oil as function of separator
            efficiecny and resident time.
eq10 = z[15] - z[12]*exp(-p.Sep_g*((z[30]*p.V_max)/ \
        ((p.m_max*z[5])/(p.rho_max*z[31])))) # Mass
            fraction of gas as function of separator
            efficiecny and resident time.
eq11 = z[21] + z[22]  - 1 # mass fractions equal to 1 for
    stream 5
eq12 = z[15] + z[16] + z[17] - 1 # mass fractions equal to
     1 for stream 3
eq13 = u[0] - z[29] # No pressure drop over the separator
eq14 = z[27] - u[0] - (p.rho_max/p.P_max)*z[31]*p.g*u[1]*(
```

```
    p.Pa_Bar) # Pressure in outlet stream 3 [bar]
eq15 = z[31] - (p.rho_w/p.rho_max)*( z[15]*p.SG_g + z[16]*
    p.SG_o + z[17]*p.SG_w) # Density stream 3 [kt/m^3]
eq16 = z[32] - (p.rho_w/p.rho_max)*(z[21]*p.SG_g + z[22]*p
    .SG_o )
eq17 = z[30] - p.L*((u[1] - p.R)*sqrt(2*p.R*u[1]-u[1]**2)
    \
                + p.R**2*acos(1-u[1]/p.R))*(1/p.V_max) #
                    Volume of liquid in the separator [m
                    ^3]


# Valve2
eq18 = z[5] - z[6] # Mass balance over valve [kt/tau]
eq19 = z[6] - (p.u1*p.Cv1/p.m_max)*sqrt((p.P_max*(z[27]-z
    [28]))/(z[15]*p.SG_g \
                + z[16]*p.SG_o + z[17]*p.SG_w)) # Mass
                    flow out of the valve
eq20 = z[15] - z[18] # Mass fraction constant over valve
eq21 = z[16] - z[19] # Mass fraction constant over valve
eq22 = z[17] - z[20] # Mass fraction constant over valve


# Compressor
eq23 = z[7] - z[8] # mass flow constant over compressor
eq24 = z[21] - z[23] # Mass fraction constant over
    compressor
eq25 = z[22] - z[24] # Mass fraction constant over
    compressor
eq26 = u[2] - (p.gamma/(p.gamma - 1))*((p.Rg*p.Ts/p.M)*((z
    [33]/z[29])**((p.gamma-1)/p.gamma) \
                -1))*((z[7]*p.m_max)/(p.W_max*x[1]))
                    *(1.1574e-6) # Compressor duty [MW]


if i == 0:
        Sol_z = vertcat(eq30,eq28,eq29,eq31,eq1,eq6,eq18,
            eq7,eq23,
                                eq32,eq33,eq34,eq3,eq4,eq5
                                    ,eq10,eq8,eq12,
                                eq20,eq21,eq22,eq11,eq9,
                                    eq24,eq25,
                                eq27,eq2,eq14,eq19,eq13,
                                eq17,eq15,eq16,eq26)

        f_z = Function("f_z",[z],[Sol_z])

        Z_0 = [0.843983, 0.0845017, 0.0132034, 0.941688,
            0.941688, 0.0632842, 0.0632842, 0.878404,
            0.878404,
                0.896245, 0.0897343, 0.014021, 0.896245,
                    0.0897343, 0.014021, 1.03142e-009,
                    0.791364, 0.208636,
                1.03142e-009, 0.791364, 0.208636,
                    0.960814, 0.0391857, 0.960814,
                    0.0391857,
                0.564091, 0.501066, 0.351623, 0.350759,
```

```
                                    0.35,
                                0.708209, 0.920864, 0.707837, 0.70372]

                        s = rootfinder("s", "kinsol", f_z)

                        Z_init = s(Z_0)

                    # Integrate over the element
                    Ik = Int( x0=X_init, z0=Z_init, p=U_init)

                    temp_x = casadi_vec(dae_x,1.0,Pr=X_init[0],eta=X_init[1])
                    temp_xc = Ik['xf'][:,1:p.d+1]
                    temp_z = Ik['zf'][:,1:p.d+1]
                    temp_u = casadi_vec(dae_u,1.0,P2=U_init[0],h=U_init[1],Ws=
                        U_init[2])
                    init.append(casadi_vec(V_block,0.0,X=temp_x,XC=temp_xc,Z=
                        temp_z,U=temp_u))

                    # Output for x and z
                    xfin = Ik['xf']
                    zfin = Ik['zf']
                    X_init = xfin[:,p.d]
                    Z_init = zfin[:,p.d]

                    if i == p.N-1:
                            init.append(casadi_vec(dae_x,1.0,Pr=X_init[0],eta=
                                X_init[1]))

        init = vertcat(*init)

        return init
```

D.4 Structure

```
from math import pi
from casadi import *
import numpy as np
from collections import OrderedDict
from helpers import casadi_vec, casadi_struct, casadi_vec2struct,
    casadi_struct2vec

def Layout(p,f,dx,obj,x,z,u,t_end):

        dae_int = {'x':x, 'z':z, 'p':u, 't':t_end, 'ode':dx, 'alg':f, '
            quad':obj}

        ts = ([0] + collocation_points(p.d, 'radau') )
        t = [q/p.N for q in ts]
        opts = {}
        opts['abstol'] = 1e-8 # abs. tolerance
        opts['reltol'] = 1e-8 # rel. tolerance
        opts['linear_solver'] = 'csparse'
        opts['linear_solver_type'] = 'user_defined'
        opts['grid'] = t
        opts['output_t0'] = True
        Int = integrator('Int', 'idas', dae_int, opts)
```

```
        # Make dictionary for variables and equations
        dae_x = OrderedDict()
        dae_z = OrderedDict()
        dae_u = OrderedDict()
        dae_t_end = OrderedDict()
        for k in range(x.shape[0]):
                dae_x.update({str(x[k]):x[k]})
        for j in range(z.shape[0]):
                dae_z.update({str(z[j]):z[j]})
        for i in range(u.shape[0]):
                dae_u.update({str(u[i]):u[i]})


        dae = {}
        dae["x"] = casadi_struct2vec(dae_x)
        dae["z"] = casadi_struct2vec(dae_z)
        dae["p"] = casadi_struct2vec(dae_u)
        if p.On == 1:
                dae_t_end.update({'t_end':t_end})
                dae["t_end"] = casadi_struct2vec(dae_t_end);
        dae["ode"] = dx
        dae["alg"] = f
        dae["quad"] = obj

        # Get collocation points
        tau_root = [0] + collocation_points(p.d, 'radau')

        return Int,dae,dae,dae_x,dae_z,dae_u,tau_root,dae_t_end
```

D.5 Collocation Method

```
from casadi import *

def simpleColl(dae,tau_root,h):

        daefun = Function("fun",dae,["x","z","p","t_end"],["ode","alg","
            quad"])

        daefun.expand()
        # Degree of interpolating polynomial
        d = len(tau_root)-1

        # Coefficients of the collocation equation
        C = np.zeros((d+1,d+1))

        # Coefficients of the continuity equation
        D = np.zeros(d+1)

        # Dimensionless time inside one control interval
        tau = SX.sym("tau")

        # For all collocation points
        for j in range(d+1):
                # Construct Lagrange polynomials to get the polynomial
```

```
            basis at the collocation point
        L = 1
        for r in range(d+1):
            if r != j:
                L *= (tau-tau_root[r])/(tau_root[j]-
                    tau_root[r])
        lfcn = Function('lfcn', [tau],[L])

        # Evaluate the polynomial at the final time to get the
            coefficients of the continuity equation
        D[j] = lfcn(1.0)

        # Evaluate the time derivative of the polynomial at all
            collocation points to get the coefficients of the
            continuity equation
        tfcn = lfcn.tangent()
        for r in range(d+1):
          C[j,r], _ = tfcn([tau_root[r]])

# State variable
CVx  = MX.sym("x",dae["x"].size1(),1)

# Helper state variables
CVCx  = MX.sym("x",dae["x"].size1(),d)

# Algebraic variables
CVz  = MX.sym("z",dae["z"].size1(),d)

# Fixed parameters (controls)
CVp  = MX.sym("p",dae["p"].size1())

# End time
t_end  = MX.sym('t_end',1);

X = horzcat(CVx,CVCx)
g = []
quad_k = 0.0
# For all collocation points
for j in range(1,d+1):

        # Get an expression for the state derivative at the
            collocation point
        xp_jk = 0
        for r in range (d+1):
            xp_jk += C[r,j]*X[:,r]

        # Add collocation equations to the NLP
        if j < d:
            [ode,alg,_] = daefun(CVCx[:,j-1],CVz[:,j-1],CVp,
                t_end)
        else: # Only add the cost function at the end of the
            element
            [ode,alg,quad] = daefun(CVCx[:,j-1],CVz[:,j-1],CVp
                ,t_end)
            quad_k += quad
        g.append(h*ode - xp_jk)
        g.append(alg)
```

```
        # Get an expression for the state at the end of the finite element
        xf_k = 0
        for r in range(d+1):
                xf_k += D[r]*X[:,r]

        G = Function("G",[CVx,CVCx,CVz,CVp,t_end],[xf_k,vertcat(*g),quad_k
            ])

        return G
```

D.6 Deterministic Optimization

```
from math import pi
from casadi import *
import numpy as np
import matplotlib.pyplot as plt
from collections import OrderedDict
from helpers import casadi_vec, casadi_struct, casadi_vec2struct,
    casadi_struct2vec
from Parameters import Parameters # Import the parameters
from Model import Model # Import the model equations
from Layout import Layout # Import the integrator, structure and timegrid
from Initial import Initial # Import the initial guess

p = Parameters();
[f,dx,obj,x,z,u,t_end] = Model(p);
[Int,dae,dae,dae_x,dae_z,dae_u,tau_root,dae_t_end] = Layout(p,f,dx,obj,x,z
    ,u,t_end);

def demopt(dae_x,dae_z,dae_u,dae,p,z):
        # Import collocation script
        from collocation_tools import simpleColl
        if p.On == 1:
                from collocation_tools_t import simpleColl
        else:
                from collocation_tools import simpleColl
        collfun = simpleColl(dae,tau_root,1.0/p.N)
        collfun = collfun.expand()
        # Number of varibles
        nx = dae["x"].shape[0] # Differential variables
        nu = dae["p"].shape[0] # Control variables
        nz = dae["z"].shape[0] # Algebraic variables
        nvar = nx + nx*p.d + nz*p.d + nu # number of variables
        nv = nx*(p.N+1) + nx*p.d*p.N + nz*p.d*p.N + nu*p.N # Total number
            of variables

        Xs  = [MX.sym("X",nx) for i in range(p.N+1)]
        XCs = [MX.sym("XC",nx,p.d) for i in range(p.N)]
        Zs  = [MX.sym("Z",nz,p.d) for i in range(p.N)]
        Us  = [MX.sym("U",nu) for i in range(p.N)]
        if p.On == 1:
                t_end = MX.sym("t_end")
        V_block = OrderedDict()
        V_block["X"]  = Sparsity.dense(nx,1)
        V_block["XC"] = Sparsity.dense(nx,p.d)
```

```
V_block["Z"]  = Sparsity.dense(nz,p.d)
V_block["U"]  = Sparsity.dense(nu,1)

# Simple bounds on states
lbx = [];
ubx = [];

# Objective function
f = 0.0;

# List of constraints
g = [];

# List of all decision variables (determines ordering)
V = [];

for k in range(p.N):
        # Add decision variables
        V += [casadi_vec(V_block,X=Xs[k],XC=XCs[k],Z=Zs[k],U=Us[k
            ])]

        if k==0:
                # Bounds at t=0
                x_lb = casadi_vec(dae_x,0.0,Pr=1.0,eta=1.0)
                x_ub = casadi_vec(dae_x,1.0,Pr=1.0,eta=1.0)
                xc_lb = casadi_vec(dae_x,0.0,eta=0.80)
                xc_lb = repmat(xc_lb,1,p.d)
                xc_ub = casadi_vec(dae_x,1.0)
                xc_ub = repmat(xc_ub,1,p.d)
                u_lb = casadi_vec(dae_u,0.0,P2=0.2,h=0.5)
                u_ub = casadi_vec(dae_u,1.0,h=2.5)
                z_lb = casadi_vec(dae_z,0.0,P6=0.48)
                z_lb = repmat(z_lb,1,p.d)
                z_ub = casadi_vec(dae_z,1.0,Z5_o=0.01,Z3_g=0.1)
                z_ub = repmat(z_ub,1,p.d)
                lbx.append(casadi_vec(V_block,-inf,X=x_lb,XC=xc_lb
                    ,Z=z_lb,U=u_lb))
                ubx.append(casadi_vec(V_block,inf,X=x_ub,XC=xc_ub,
                    Z=z_ub,U=u_ub))
        else:
                # Bounds for other t
                x_lb = casadi_vec(dae_x,0.0,eta=0.80)
                x_ub = casadi_vec(dae_x,1.0)
                xc_lb = casadi_vec(dae_x,0.0,eta=0.80)
                xc_lb = repmat(xc_lb,1,p.d)
                xc_ub = casadi_vec(dae_x,1.0)
                xc_ub = repmat(xc_ub,1,p.d)
                u_lb = casadi_vec(dae_u,0.0,P2=0.2,h=0.5)
                u_ub = casadi_vec(dae_u,1.0,h=2.5)
                z_lb = casadi_vec(dae_z,0.0,P6=0.48)
                z_lb = repmat(z_lb,1,p.d)
                z_ub = casadi_vec(dae_z,1.0,Z5_o=0.01,Z3_g=0.1)
                z_ub = repmat(z_ub,1,p.d)
                lbx.append(casadi_vec(V_block,-inf,X=x_lb,XC=xc_lb
                    ,Z=z_lb,U=u_lb))
                ubx.append(casadi_vec(V_block,inf,X=x_ub,XC=xc_ub,
                    Z=z_ub,U=u_ub))
```

```
        # Obtain collocation expressions
        if p.On == 1:
                # Varying time horizon
                [Xnext,constr,quad_k] = collfun(Xs[k],XCs[k],Zs[k
                    ],Us[k],t_end)
        else:
                # Fixed time horizon
                [Xnext,constr,quad_k] = collfun(Xs[k],XCs[k],Zs[k
                    ],Us[k])
        g.append(constr) # Add algebraic constraints
        g.append(Xs[k+1] - Xnext) # Add continuity constraint
            added
        # Add to the objective function
        if p.PV == 1:
                # Present Value is included
                f += quad_k/(1.05)**(k*t_end/12.0)
        else:
                # Present Value is not included
                f += quad_k

V += [Xs[-1]]

if p.On == 1:
        # Add time horizon as varible for varying time horizin
        V += [t_end]
        f *= V[-1]

# Bounds for final t
x_lb = casadi_vec(dae_x,0.0,eta=0.80)
x_ub = casadi_vec(dae_x,1.0)
lbx.append(x_lb)
ubx.append(x_ub)

if p.On == 1:
        # Add constraint on end time horizon
        t_lb = casadi_vec(dae_t_end,0.8)
        t_ub = casadi_vec(dae_t_end,1.2)
        lbx.append(t_lb)
        ubx.append(t_ub)

#Initial guess
init = Initial(p,z,V_block);
if p.On == 1:
        V0 = np.zeros(init.shape[0]+1)
else:
        V0 = np.zeros(init.shape[0])

for q in range(init.shape[0]):
        V0[q] = init[q]
if p.On == 1:
        V0[-1] += 1.0 # End time initial guess

# Convert constraints to lists
lbg = np.zeros(vertcat(*g).shape[0]).tolist()
ubg = np.zeros(vertcat(*g).shape[0]).tolist()
lbx = vertcat(*lbx)
ubx = vertcat(*ubx)
```

```
        nlp = {'x':vertcat(*V),'f':f, 'g':vertcat(*g)}

        options = {}
        options['warn_initial_bounds'] = True
        options['ipopt.linear_solver'] = 'ma27'
        options['ipopt.max_iter'] = 1000
        solver = nlpsol('solver','ipopt', nlp, options)

        sol = solver(x0=V0, lbx=lbx, ubx=ubx, lbg=lbg, ubg=ubg)

        # Extract all of the decision variables from the solved nlp
        v_opt = sol['x']
        if p.On == 1:
                tf = v_opt[-1]
                print tf*p.TF
        else:
                tf = p.TF
        return v_opt,nvar,lbx,ubx,tf


# [v_opt,nvar,lbx,ubx,tf] = demopt(dae_x,dae_z,dae_u,dae,p,z);
```

D.7 Stochastic Optimization

```
from math import pi
from casadi import *
import numpy as np
import matplotlib.pyplot as plt
import matplotlib.mlab as mlab
from scipy.stats import norm
from scipy.stats import invgauss
from collections import OrderedDict
from helpers import casadi_vec, casadi_struct, casadi_vec2struct,
    casadi_struct2vec
from Parameters import Parameters # Script for all of the parameters
from Model import Model # Script for the model equations
from Layout import Layout # Script for structure of the DAE system
from demopt import demopt # Deterministic optimization script
from Initial import Initial # The initial guess script

p = Parameters();
[f,dx,obj,x,z,u,t_end] = Model(p);
[Int,dae,dae,dae_x,dae_z,dae_u,tau_root,dae_t_end] = Layout(p,f,dx,obj,x,z
    ,u,t_end);
[v_opt,nvar,lbx,ubx,tf] = demopt(dae_x,dae_z,dae_u,dae,p,z);

p.TF = float(v_opt[-1])*p.TF
p.On = 0

[f,dx,obj,x,z,u,t_end] = Model(p);
[Int,dae,dae,dae_x,dae_z,dae_u,tau_root,dae_t_end] = Layout(p,f,dx,obj,x,z
    ,u,t_end);
# Import collocation script
from collocation_tools import simpleColl
if p.On == 1:
```

```
        from collocation_tools_t import simpleColl
else:
        from collocation_tools import simpleColl
collfun = simpleColl(dae,tau_root,1.0/p.N)
collfun = collfun.expand()


def MonteCarlo(p,v_opt,nvar):
        """This is a function that runs the Monte Carlo simulations.
        """
        U_init = []
        for i in range(p.N):
                U_init.append(v_opt[(p.tz+i*nvar):(p.tz+3+i*nvar)])

        U_init = vertcat(*U_init)
        X_out1 = []
        Z_out1 = []
        for i in range(p.ns):

                # Generates random outcomes for ko
                if i == 0:
                        ko = p.ko
                mu_ko = ko # Mean value of the reservoir flow coefficient
                    of oil
                sigma_ko = 0.1*ko # Variance of the reservoir flow
                    coefficient of oil
                k_o = np.random.normal(mu_ko, sigma_ko)
                p.ko = k_o #

                # Update the model with new value of ko

                [f,dx,obj,x,z,u,t_end] = Model(p);

                dae_int = {'x':x, 'z':z, 'p':u,  'ode':dx, 'alg':f, 'quad'
                    :obj}

                opts = {}
                opts['abstol'] = 1e-8# abs. tolerance
                opts['reltol'] = 1e-8 # rel. tolerance
                opts['linear_solver'] = 'csparse'
                opts['linear_solver_type'] = 'user_defined'
                opts['tf'] = 1.0/p.N
                INT = integrator('INT', 'idas', dae_int, opts)

                X_out = []
                Z_out = []
                for j in range(p.N):

                        if j == 0:

                                sim = INT( x0=v_opt[0:2], z0=v_opt[p.tx:p.
                                    tx+34], p=U_init[0:3])
                                xfin = sim['xf']
                                zfin = sim['zf']

                                X_init = xfin
                                Z_init = zfin
```

```
                                X_out.append(X_init)
                                Z_out.append(Z_init)
                        else:

                                sim = INT( x0=X_init, z0=Z_init, p=U_init[
                                    j*3:j*3+3])
                                xfin = sim['xf']
                                zfin = sim['zf']
                                X_init = xfin
                                Z_init = zfin


                                X_out.append(X_init)
                                Z_out.append(Z_init)

                X_out1.append(vertcat(*X_out))
                Z_out1.append(vertcat(*Z_out))

        X_sim = np.hstack(X_out1)
        Z_sim = np.hstack(Z_out1)
        p.ko = ko

        return X_sim, Z_sim


def backoff(X_out, Z_out):
        """ This script calculates the backoff for the chance constraint
        """
        alpha_eta = 0.95 # probability level of eta
        alpha_Z3_g = 0.95 # probability level of Z5_o
        alpha_P_6 = 0.95 # probability level of P_6

        mu_eta = np.zeros(p.N) # Make the mean value matrix
        mu_Z3_g = np.zeros(p.N) # Make the mean value matrix
        mu_P_6 = np.zeros(p.N) # Make the mean value matrix

        sigma_eta = np.zeros(p.N) # Make the variance matrix
        sigma_Z3_g = np.zeros(p.N) # Make the variance matrix
        sigma_P_6 = np.zeros(p.N) # Make the variance matrix

        back_off_eta = np.zeros(p.N) # Make the back_off matrix for eta
        back_off_Z3_g = np.zeros(p.N) # Make the back_off matrix for Z5_o
        back_off_P_6 = np.zeros(p.N) # Make the back_off matrix for P_6

        for i in range(p.N):

                # Calculates the back off for each timestep
                [mu_eta[i], sigma_eta[i]] = norm.fit(X_out[i*2+1,:]) #
                    Normalfit the outcome of eta
                [mu_Z3_g[i], sigma_Z3_g[i]] = norm.fit(Z_out[i*34+15,:]) #
                     Normalfit the outcome of Z3_g
                [mu_P_6[i], sigma_P_6[i]] = norm.fit(Z_out[i*34+33,:]) #
                    Normalfit the outcome of P_6


                back_off_eta[i] = norm.ppf(alpha_eta)*sqrt(np.cov(X_out[i
                    *2+1,:])) # calculates the back off of eta
```

```
            back_off_Z3_g[i] = norm.ppf(alpha_Z3_g)*sqrt(np.cov(Z_out[
                i*34+15,:])) # calculates the back off of Z3_g

            back_off_P_6[i] =  norm.ppf(alpha_P_6)*sqrt(np.cov(Z_out[i
                *34+33,:])) # calculates the back off of P_6

        return back_off_eta, back_off_Z3_g, back_off_P_6, mu_eta, mu_Z3_g,
            mu_P_6, sigma_eta, sigma_Z3_g, sigma_P_6

[X_out, Z_out] = MonteCarlo(p, v_opt, nvar);

[back_off_eta, back_off_Z3_g, back_off_P_6, mu_eta, mu_Z3_g, mu_P_6, sigma_eta,
    sigma_Z3_g, sigma_P_6] = backoff(X_out, Z_out);

BO_eta = back_off_eta.tolist()
BO_Z3_g = back_off_Z3_g.tolist()
BO_P6 = back_off_P_6.tolist()

def StochOpt(p, v_opt, nvar, BO_P6, BO_Z3_g, BO_eta):

        # Import collocation script
        from collocation_tools import simpleColl
        if p.On == 1:
                from collocation_tools_t import simpleColl
        else:
                from collocation_tools import simpleColl
        collfun = simpleColl(dae, tau_root, 1.0/p.N)
        collfun = collfun.expand()
        # Number of varibles
        nx = dae["x"].shape[0] # Differential variables
        nu = dae["p"].shape[0] # Control variables
        nz = dae["z"].shape[0] # Algebraic variables
        nvar = nx + nx*p.d + nz*p.d + nu # number of variables
        nv = nx*(p.N+1) + nx*p.d*p.N + nz*p.d*p.N + nu*p.N # Total number
            of variables

        Xs  = [MX.sym("X",nx) for i in range(p.N+1)]
        XCs = [MX.sym("XC",nx,p.d) for i in range(p.N)]
        Zs  = [MX.sym("Z",nz,p.d) for i in range(p.N)]
        Us  = [MX.sym("U",nu) for i in range(p.N)]
        if p.On == 1:
                t_end = MX.sym("t_end")
        V_block = OrderedDict()
        V_block["X"]  = Sparsity.dense(nx,1)
        V_block["XC"] = Sparsity.dense(nx,p.d)
        V_block["Z"]  = Sparsity.dense(nz,p.d)
        V_block["U"]  = Sparsity.dense(nu,1)

        # Simple bounds on states
        lbx = [];
        ubx = [];

        # Objective function
        f = 0.0;

        # List of constraints
```

```
g = [];

# List of all decision variables (determines ordering)
V = [];

for k in range(p.N):
        # Add decision variables
        V += [casadi_vec(V_block,X=Xs[k],XC=XCs[k],Z=Zs[k],U=Us[k
            ])]

        if k==0:
                # Bounds at t=0
                x_lb = casadi_vec(dae_x,0.0,Pr=1.0,eta=1.0)
                x_ub = casadi_vec(dae_x,1.0,Pr=1.0,eta=1.0)
                xc_lb = casadi_vec(dae_x,0.0,eta=0.80)
                xc_lb = repmat(xc_lb,1,p.d)
                xc_ub = casadi_vec(dae_x,1.0)
                xc_ub = repmat(xc_ub,1,p.d)
                u_lb = casadi_vec(dae_u,0.0,P2=0.2,h=0.5)
                u_ub = casadi_vec(dae_u,1.0,h=2.5)
                z_lb = casadi_vec(dae_z,0.0,P6=0.48 )
                z_lb = repmat(z_lb,1,p.d)
                z_ub = casadi_vec(dae_z,1.0,Z5_o=0.01,Z3_g=0.1 -
                    BO_Z3_g[k])
                z_ub = repmat(z_ub,1,p.d)
                lbx.append(casadi_vec(V_block,-inf,X=x_lb,XC=xc_lb
                    ,Z=z_lb,U=u_lb))
                ubx.append(casadi_vec(V_block,inf,X=x_ub,XC=xc_ub,
                    Z=z_ub,U=u_ub))
        else:
                # Bounds for other t
                x_lb = casadi_vec(dae_x,0.0,eta=0.80)
                x_ub = casadi_vec(dae_x,1.0)
                xc_lb = casadi_vec(dae_x,0.0,eta=0.80)
                xc_lb = repmat(xc_lb,1,p.d)
                xc_ub = casadi_vec(dae_x,1.0)
                xc_ub = repmat(xc_ub,1,p.d)
                u_lb = casadi_vec(dae_u,0.0,P2=0.2,h=0.5)
                u_ub = casadi_vec(dae_u,1.0,h=2.5)
                z_lb = casadi_vec(dae_z,0.0,P6=0.48 )
                z_lb = repmat(z_lb,1,p.d)
                z_ub = casadi_vec(dae_z,1.0,Z5_o=0.01,Z3_g=0.1 -
                    BO_Z3_g[k])
                z_ub = repmat(z_ub,1,p.d)
                lbx.append(casadi_vec(V_block,-inf,X=x_lb,XC=xc_lb
                    ,Z=z_lb,U=u_lb))
                ubx.append(casadi_vec(V_block,inf,X=x_ub,XC=xc_ub,
                    Z=z_ub,U=u_ub))
        # Obtain collocation expressions
        if p.On == 1:
                # Varying time horizon
                [Xnext,constr,quad_k] = collfun(Xs[k],XCs[k],Zs[k
                    ],Us[k],t_end)
        else:
                # Fixed time horizon
                [Xnext,constr,quad_k] = collfun(Xs[k],XCs[k],Zs[k
                    ],Us[k])
```

```
            g.append(constr) # Add algebraic constraints
            g.append(Xs[k+1] - Xnext) # Add continuity constraint
                added
            # Add to the objective function
            if p.PV == 1:
                    # Present Value is included
                    f += quad_k/(1.05)**(k*1.0/12.0)
            else:
                    # Present Value is not included
                    f += quad_k

    V += [Xs[-1]]

    if p.On == 1:
            # Add time horizon as varible for varying time horizin
            V += [t_end]
            f *= V[-1]

    # Bounds for final t
    x_lb = casadi_vec(dae_x,0.0,eta=0.8 + BO_eta[-1])
    x_ub = casadi_vec(dae_x,1.0)
    lbx.append(x_lb)
    ubx.append(x_ub)

    if p.On == 1:
            # Add constraint on end time horizon
            t_lb = casadi_vec(dae_t_end,0.8)
            t_ub = casadi_vec(dae_t_end,1.2)
            lbx.append(t_lb)
            ubx.append(t_ub)

    #Initial guess
    init = Initial(p,z,V_block);
    if p.On == 1:
            V0 = np.zeros(init.shape[0]+1)
    else:
            V0 = np.zeros(init.shape[0])

    for q in range(init.shape[0]):
            V0[q] = init[q]
    if p.On == 1:
            V0[-1] += 1.0 # End time initial guess

    # Convert constraints to lists
    lbg = np.zeros(vertcat(*g).shape[0]).tolist()
    ubg = np.zeros(vertcat(*g).shape[0]).tolist()
    lbx = vertcat(*lbx)
    ubx = vertcat(*ubx)

    nlp = {'x':vertcat(*V),'f':f, 'g':vertcat(*g)}

    options = {}
    options['warn_initial_bounds'] = True
    options['ipopt.linear_solver'] = 'ma27'
    options['ipopt.max_iter'] = 1000
    solver = nlpsol('solver','ipopt', nlp, options)
```

```
        sol = solver(x0=V0, lbx=lbx, ubx=ubx, lbg=lbg, ubg=ubg)

        # Extract all of the decision variables from the solved nlp
        v_opt = sol['x']
        if p.On == 1:
                tf = v_opt[-1]
                print tf*p.TF
        else:
                tf = p.TF

        [X_out,Z_out] = MonteCarlo(p,v_opt,nvar)

        return v_opt,X_out,Z_out,

[v_opt,X_out,Z_out] = StochOpt(p,v_opt,nvar,BO_P6,BO_Z3_g,BO_eta);

[back_off_eta, back_off_Z3_g,back_off_P_6,mu_eta,mu_Z3_g,mu_P_6,sigma_eta,
    sigma_Z3_g,sigma_P_6] = backoff(X_out,Z_out);
```